INFORMATION TO USERS

This reproduction was made from a copy of a document sent to us for microfilming. While the most advanced technology has been used to photograph and reproduce this document, the quality of the reproduction is heavily dependent upon the quality of the material submitted.

The following explanation of techniques is provided to help clarify markings or notations which may appear on this reproduction.

1. The sign or "target" for pages apparently lacking from the document photographed is "Missing Page(s)". If it was possible to obtain the missing page(s) or section, they are spliced into the film along with adjacent pages. This may have necessitated cutting through an image and duplicating adjacent pages to assure complete continuity.

2. When an image on the film is obliterated with a round black mark, it is an indication of either blurred copy because of movement during exposure, duplicate copy, or copyrighted materials that should not have been filmed. For blurred pages, a good image of the page can be found in the adjacent frame. If copyrighted materials were deleted, a target note will appear listing the pages in the adjacent frame.

3. When a map, drawing or chart, etc., is part of the material being photographed, a definite method of "sectioning" the material has been followed. It is customary to begin filming at the upper left hand corner of a large sheet and to continue from left to right in equal sections with small overlaps. If necessary, sectioning is continued again — beginning below the first row and continuing on until complete.

4. For illustrations that cannot be satisfactorily reproduced by xerographic means, photographic prints can be purchased at additional cost and inserted into your xerographic copy. These prints are available upon request from the Dissertations Customer Services Department.

5. Some pages in any document may have indistinct print. In all cases the best available copy has been filmed.

University Microfilms International

300 N. Zeeb Road
Ann Arbor, MI 48106

8312384

Wang, Chao-Yea R.

LARGE SCALE GALACTIC SHOCKS AND MOTIONS OF THE CLOUD MEDIUM

City University of New York PH.D. 1983

University
Microfilms
International 300 N. Zeeb Road, Ann Arbor, MI 48106

Copyright 1983

by

Wang, Chao-Yea R.

All Rights Reserved

PLEASE NOTE:

In all cases this material has been filmed in the best possible way from the available copy. Problems encountered with this document have been identified here with a check mark __✓__.

1. Glossy photographs or pages _____
2. Colored illustrations, paper or print _____
3. Photographs with dark background _____
4. Illustrations are poor copy _____
5. Pages with black marks, not original copy _____
6. Print shows through as there is text on both sides of page _____
7. Indistinct, broken or small print on several pages ✓
8. Print exceeds margin requirements _____
9. Tightly bound copy with print lost in spine _____
10. Computer printout pages with indistinct print _____
11. Page(s) _____ lacking when material received, and not available from school or author.
12. Page(s) _____ seem to be missing in numbering only as text follows.
13. Two pages numbered _____. Text follows.
14. Curling and wrinkled pages _____
15. Other _____

University
Microfilms
International

LARGE SCALE GALACTIC SHOCKS AND MOTIONS OF THE CLOUD MEDIUM

by

CHAO-YEA . WANG

A dissertation submitted to
the Graduate Faculty in Physics
in partial fulfillment of the requirements
for the degree of Doctor of Philosophy,
The City University of New York.

1983

This manuscript has been read and accepted for the Graduate Faculty in Physics in satisfaction of the dissertation requirement for the degree of Doctor of Philosophy.

1-31-83
date

Chairman of Examining Committee

2/28/83
date

Executive Officer

Hung-yee Chiu

Richard B. Stetner

Supervisory Committee

The City University of New York

Abstract

LARGE SCALE GALACTIC SHOCKS AND

MOTIONS OF THE CLOUD MEDIUM

by

CHAO-YEA . WANG

Adviser: Professor Chi Yuan

Quasi-steady flows of the interstellar gas in a spiral gravitational field are studied for the purpose of further understanding galactic shock, interstellar clouds, and star formation in the post shock regions.

Qualitatively,we closely follow the two-phase model explored by Shu et al . (1972). Moreover, we extend the field of investigation to the cloud phase in the post shock regions, especially where the star formation and cloud-cloud collisions are prominent. The problem also includes the velocity difference between the cloud and intercloud phases behind the shock front. We demonstrate that the drag force between the cloud and the intercloud phase is far from sufficient enough to bring them to co-move within a reasonable distance behind the shock front. We then further study the behavior of the cloud-cloud collision and conclude that the cloud-cloud collision is the major mechanism that slows down the velocity

of clouds in the post shock regions within approximately 100pc behind the shock front.

We also determine the structure of the shock layer of the cloud medium. The kinematic turbulence viscosity is assumed to be equal to the product of the mean free path of the cloud-cloud collision and the mean turbulence speed of clouds.

By adopting the equation of state of the interstellar gas, we can carry out a detailed study of Quasi-steady flows of interstellar gas including phase transition. Our results are in good agreement with the results of Shu et al. (1972). In 1976 De Jong proposed that in addition to the low-energy cosmic rays, photoelectric heating is a major heating source for the interstellar gas. He then determined the equation of state for the interstellar gas that is in better agreement with existing observations.

We use De Jong's equation of state for the interstellar gas and repeat similar calculations to those done by Shu et al. (1972). Our results again agree with Shu et al . (1972).

ACKNOWLEDGEMENTS

The following have provided crucial assistance and support throughout my course of study:

Professor Chi Yuan who gave me valued instruction and guidance, countless encouragement and assistance;

Professor Robert Lea and professor M.P. Sarachik, both of whom gave me greatly needed advice and assistance;

Professor Hong-Yee Chiu and professor Richard Stothers , who provided invaluable assistance, advice, and hospitality at Goddard Institute for space studies;

Professor Leon Cohen and professor M. L. West, both of whom gave sound advice and followed the writing of my thesis with interest and understanding;

And my wife Grace whose understanding, moral support and help in preparing the manuscript is greatly appreciated.

Much thanks to all.

TABLE OF CONTENTS

	page
APPROVAL PAGE	ii
ABSTRACT	iii
ACKNOWLEDGEMENTS	vii
TABLE OF CONTENTS	viii
LIST OF TABLES	x
LIST OF FIGURES	xi
CHAPTER I: HISTORICAL BACKGROUND AND DEFINING THE PROBLEM	
I-a Introduction	2
I-b Structure of the Thesis	15
CHAPTER II: DOUBLY PERIODIC SHOCK SOLUTIONS OF THE INTERCLOUD MEDIUM	
II-a Galactic Shocks in an Interstellar Medium with Two Stable Phases as Proposed by Shu *et al*	18
II-b Comfirmation of the Results of Shu *et al*	25
II-c Doubly Periodic Shock Solutions for the Two-Phase Model of Interstellar Gas Proposed by De Jong	47
II-d Results for De Jong's Model	53

CHAPTER III: THE INABILITY OF THE DRAG FORCE IN DECELERATING THE CLOUD MEDIUM 78

CHAPTER IV : THE SHOCK STRUCTURE OF THE CLOUD MEDIUM RESULTING FROM CLOUD-CLOUD COLLISION

IV-a Structure of a Galactic Shock 90

IV-b Final State of a Galactic Shock 94

IV-c The Viscous Layer 96

Iv-d The Layer of Thermodynamic Relaxation and Phase Transition 98

IV-e The Layer of Cloud-Cloud Collisions 104

IV-f Results 114

CHAPTER V : CONCLUSIONS 127

REFERENCES 132

LIST OF TABLES

Table No.	Title	Page
1	A Glossary of Parameters Used in the Computation for Shu's Model	124
2	Numerical Values of the Principal Variables at the Four Key Locations for Shu's Model	125
3	A Glossary of Parameters Used in the Computation for De Jong's Model	126
4	Numerical Values of the Principal Variables at the Four Key Locations for De Jong's Model	127
5	Numerical Values of the Principal Variables Behind Shock Front for Shu's Model	128
6	Numerical Values of the Principal Variables Behind Shock Front for De Jong's Model	129

LIST OF FIGURES

Figure No.	Title	Page
2-1	The Procedure Used to Locate the Galactic Shock	34
2-2	The Variation of Local Sonic Speed along a Streamline Which Passes Through the Solar Neighborhood	36
2-3	The Variation of the Tangential Velocity of the Interstellar Gas Along the Entire Streamline Which Passes Through Solar Neighborhood.(Shu's Model)	38
2-4	The Variation of the Normal Velocity of the Interstellar Gas Along the Entire Streamline Which Passes Through the Solar Neighborhood.(Shu's Model)	40
2-5	The Variation of the Pressure of the Interstellar Gas Along the Entire Streamline Which Passes Through the Solar Neighborhood.(Shu's Model)	42

Figure No.	Title	Page
2-6	The Variation of the Number Density of the Intercloud Medium Along the Entire Streamline. (Shu's Model)	44
2-7	The Variation of the Local Fraction of Volume Occupied by the Cloud Medium F_c Along the Entire Streamline.(Shu's Model)	46
2-8	The Variation of the Radius of the Entire Streamline Which Passes Through the Solar Neighborhood.(Shu's Model)	48
(2-9)—(2-11)	Models of Two-Phase Interstellar Gas Which Proposed by De Jong	63
2-12	The Procedure Used to Locate the Galactic Shocks(STS Solution) for De Jong's Model.	65
2-13	The Variation of Local Sonic Speed Along a Streamline Which Passes Through the Solar Neighborhood.(De Jong's Model)	67

Figure No.	Title	Page
2-14	The Variation of the Tangential Velocity of the Interstellar Gas Along the Entire Streamline Which Passes Through Solar Neighborhood.(De Jong's Model)	69
2-15	The Variation of the Normal Velocity of the Interstellar Gas Along the Entire Streamline Which Passes Through the Solar Neighborhood. (De Jong's Model)	71
2-16	The Variation of the Pressure of the Interstellar Gas Along the Entire Streamline Which Passes Through the Solar Neighborhood.(De Jong's Model)	73
2-17	The Variation of the Number Density of the Intercloud Medium Along the Entire Streamline. (De Jong's Model)	75
2-18	The Variation of the Local Fraction of Volume Occupied by the Cloud Medium F_c Along the Entire Streamline.(De Jong's Model)	77

Figure No.	Title	Page
2-19	The Variation of the Radius of the Entire Streamline Which Passes Through the Solar Neighborhood. (De Jong's Model)	79
3-1	The Deceleration of the Cloud Medium by Drag Force Alone, and The Variations of Velocities of Both the Cloud and the Intercloud Media Behind Shock Front	91
4-1	The Variations of the Normal Velocities and Densities in the Galactic Shock for Shu's Model	120
4-2	The Variations of the Normal Velocities and Densities in the Galactic Shock for De Jong's Model	122

CHARTER I

HISTORICAL BACKGROUND AND DEFINING THE PROBLEM

I-a Introduction

The first question we encounter in the study of galaxies is how to interprete the striking phenomenon of the spiral stucture which is maintained as a relatively permanent pattern.

Decades ago B.Lindblad first attempted to interpret the spiral structure as a wave pattern; however, a detailed physical formulation was not carried out until the 1960's.

In the 60's Lin,Shu,Toomre,Kalnajs,Yuan,and Roberts proposed,in a series of papers,"the density-wave theory" to interprete the spiral structure and postulated that these spiral structures are the results of density wave pattern. A density wave pattern rotates about the center of a galaxy at a pattern speed Ω_p, while the individual stars and the interstellar gas rotate around the center of the galaxy in response to their local gravitational field. Thus the spiral pattern is relatively permanent,

yet its constituents are transient as waves pass by. The spiral arms coincide with the minimum gravitational potential of the density wave. According to density-wave theory, there is only 10% more mass in the spiral arms regions than in the interarm regions. The mass distribution of a normal galaxy is basically rotationally symmetrical. However, the following question arises: why are the spiral arms far more prominent in observation than in the interarm regions with only 10% more mass? or why do the new stars often form along two spiral arms in external spiral galaxies? This question , due to the application of the density wave theory. may be resolved through the presence of large-scale shock waves in the interstellar gas along the spiral arms. Such shock waves are capable of triggering the gravitational collapse of massive clouds along the extensive shock front.This idea was first explored by Fujimoto (1968), but the complete theory and its implications were not worked out until later by Roberts (1969). Then Roberts and Yuan (1970)

extended the theory to include the galactic magnetic field. In all these early works, a working hypothesis was made, i.e., the pressure of the interstellar medium is assumed to be the product of the average density of the clouds and the square of their average random speed. Such a description of the interstellar medium is sometimes referred to as the turbulence model. The interest at that time was to find the large-scale shock solution along the spiral arm rather than to find the structure of the shock, the behavior of the interstellar medium in the post shock region, and the complicated processes of star formation.

There is yet another question to star formation which remains to be answered. If an interstellar cloud is placed in a vacuum as an isolated entity, it is not even remotely bound by its own gravity. Thus, how can it exist permanently and, moreover, form into new stars? To answer this question, an important development was put forth by Shu et al. (1972), who solved the shock formation problem with

the two-phase model proposed by Spitzer and Scott (1969), Field, Goldsmith, and Habing(1969). The intercloud phase is considered to be a hot and rarified intercloud medium, while the cloud phase is considered to be cold, and dense interstellar clouds embedded in the intercloud medium. These two phases are in pressure balance and are moving with the same velocity (co-moving) most of the time except for a thin layer behind the shock front, where the intercloud phase experiences a galactic shock and immediately slows down into post shock subsonic velocity. Meanwhile the cloud phase still moves at supersonic speed and plunges into the subsonic intercloud phase. At the same time the interstellar clouds are being compressed by its ambient intercloud medium into star formations and are decelerating rapidly behind the shock front. The cloud phase slows down and begins co-moving with the intercloud phase in a short distance behind the shock front. The mechanism of deceleration was not worked out in the paper by Shu et al. However, they suggested that "in the shock

layer the clouds are initially decelerated by the drag exerted by the intercloud medium and suffer further deceleration because cloud-cloud collisions serve as an effective means of(diffusive) momentum transport in regions where the gradient of the bulk velocity is large". The analysis was carried out only for the intercloud medium in the work of Shu et al. The cloud medium was assumed to have the same speed of the intercloud medium even at the location of the shock. Shu et al. therefore obtained the "outer solution" to the equations of the two-phase gas medium in the convention of fluid mechanics. The shock layer, however, was treated as infinitesimally thin for both media.

Two interesting studies following the line of approach of Shu et al. were made afterwards. Sawa(1975) started to look into the detailed behavior of the cloud medium in the post-shock regions of the intercloud medium using the same equations of Shu et al., but he added

a term of eddy viscosity due to the turbulence in the intercloud medium. He only treated the normal component of the intercloud medium and managed to obtain a solution for the cloud medium in the post-shock regions. The distance between the shock and the location where the cloud medium starts to move together again with the intercloud medium is about 70° in terms of the phase angle or about 700pc normal to the shock of the galacto-centric distance of 10kpc. Sawa's work has severe shortcomings. First, he only treated the one-dimensional problem while neglecting the velocity component parallel to the shock front that undergoes substantial changes under the influence of the Coriolis force over a distance of 700pc normal to the shock. The tangential velocity difference between these two phases in our calculations is of the order of 8km/sec(see Figure 3-1) which introduce two uneven Coriolis forces along the normal direction for each of the two phases. These two Coriolis forces push the two phases further apart instead of getting them to move together. This result

convinces us that the drag force between the two phases is not the main mechanism that brings them to co-move.Possible exceptions are clouds much smaller than the average cloud(Spitzer 1968). Second, the drag force acts on both the cloud medium and the intercloud medium; but Sawa took only the drag force on the cloud into account. Third,the Stokes formula in his formulation does not hold for the supersonically moving clouds.

Another interesting development was made by Woodward (1976) using his elaborate computations of a single cloud entering the shock front of the intercloud medium. He demonstrated the detailed process that a cloud might go through in a galactic shock. One of his important conclusions was that the deceleration rate of a standard cloud (Spitzer 1968) is about 0.25km/sec-million years, which means that a cloud takes 100 million years to slow down to the speed of the intercloud medium.This result is incompatible with the existing observations.

Meanwhile in the observational field, there is sufficient evidence to show that both cloud and intercloud media slow down rapidly in a pattern similar to the shock solution of the density wave theory for the intercloud medium. One of the best results was carried out by Visser (1978). His result of 21cm line observations of M81 indicate that the velocity field of HI regions along the spiral arms is in excellent agreement with the solution of the density wave theory for the intercloud medium. Owing to its greater optical depth, the cloud usually contributes more to the 21cm line emission than the intercloud medium. Therefore Visser's result strongly suggests that a shock front similar to the one for the intercloud medium must exist in the cloud medium along the spiral arms.

Observations of young stars which are believed to be newly formed out of clouds also show the similar nonlinear motions. The observations of the classical cepheids

and supergaints in the Persus arm and in the Sagittarius arm are found to deviate suddenly from a smooth rotational curve in the same manner as prescribed by the shock solution of the intercloud medium(Lin,Yuan and Roberts 1978).

Mathewson et al.(1972) studied the synchrotron radiation from the decelerated charged particles of M51. His study shows that the maximum synchrotron radiation comes from the dust lanes, which strongly suggests that the clouds together with the dust particles are concentrated in the narrow regions immediately behind the shock fronts.

These observational results clearly show that the clouds do slow down rapidly behind the shock front; yet from our previous discussions, the clouds except for the very small ones cannot be slowed down by the drag force alone(chapterIII). The co-moving between these two phases can hardly be achieved, even if we increase the proportional constant C_D to very high numbers such as 30 or

50.A major question therefore arises. What is the mechanism that effectively slows down the clouds immediately behind the shock front of intercloud medium? A re-examination of the dynamic behavior behind the shock front for these two phases therefore becomes necessary. We then consider clouds as turbulent clumps in the interstellar medium;their random motions and collisions cause momentum transport in the cloud medium and give rise to the turbulent viscosity.We demonstrate that cloud-cloud collisions serve as an effective mechanism to slow down the cloud medium and bring the cloud medium to co-move with the intercloud medium behind the shock (Yuan and Wang 1982). The governing equations with turbulent viscosity are discussed in chapter IV. We determine the "inner solutions" of these equations where the turbulent viscosity plays an important role and find that the shock layer of turbulent viscosity is of the order of 100pc. A thinner layer of phase transition about 20pc behind the shock also exists.
It is concluded that our velocity field for the cloud me-

dium is basically consistent with the velocity field for the intercloud medium determined by Shu et al. except for a narrow region of about 100pc behind the shock. This result is also consistent with the observations.

In our previous dicussions about the two-phase model of the interstellar gas, we considered the steady flux of low-energy cosmic rays to be the only heating source for interstellar gas.In order to reach an agreement with the observation of the interstellar gas,a very high flux of low-energy cosmic rays must be postulated (Field et al. 1969). This result contradicts the theoretical results of Kulsrud and Cesarsky(1971). They state that unless the density of the intercloud medium is many orders of magnitude less than that which has been generally accepted, low energy cosmic rays cannot be effectively detained within the galactic disk as we had previously expected. It means that there may not be enough low-energy cosmic rays available within the galactic disk to provide

a sufficient heating source for the interstellar gas.

Moreover, the postulated high flux density of the low-energy cosmic rays is about one order of magnitude greater than that derived from the observations of OH and HD densities in the interstellar clouds(Black& Dalgarno 1973 ; O'Donnel&Watson 1974). Therefore the two-phase model that we previously postulated may not be correct unless there are more efficient heating sources available within the galactic disk.

Watson(1972) suggested a promising heating mechanism other than low-energy cosmic rays—photoelectrons from dust grains produced by the photons of the interstellar radiation field between 1200Å and 912Å.

De Jong(1976) suggested that the heating effect of the photoelectrons from dust grains is even more efficient than the low-energy cosmic rays. However, in his model of the two-phase gas, he took both heating sources

into account. According to different cosmic ray ionization rates, ζ , and the photoelectron emission efficiency of dust grains, Y, different models of equations of states for the two-phase interstellar gas are determined. Among his models, the equation of state which best fits the observations are when the parameters $\zeta = 10^{-16} s^{-1}$ and Y=0.1. We use the equation of state of this better fitted model for the two-phase interstellar gas, and repeat calculations similar to those done by Shu et al. (1972). Our results again qualitatively agree with Shu et al.

I-b Structure of the Thesis

CHAPTER II: DOUBLY PERIODIC SHOCK SOLUTION OF THE INTERCLOUD MEDIUM

Using different parameters in our calculations, we confirm the results of Shu et al.(1972).By adopting the equation of state for the interstellar gas proposed by De Jong (1976), we repeat calculations similar to those done by Shu et at. The results are in agreement with Shu et al.1972.

CHAPTER III: THE INABILITY OF THE DRAG FORCE IN DECELERATING THE CLOUD MEDIUM

We show that the drag force between the two phases is not capable of slowing down the cloud medium so as to achieve the co-moving with the intercloud phase within a short distance behind the shock.

CHAPTER IV: THE SHOCK STRUCTURE OF THE CLOUD MEDIUM

RESULTING FROM CLOUD-CLOUD COLLISIONS

The equations for the cloud medium, when the cloud-cloud collisions are taken into account, are derived. It is demonstrated that the turbulent visicosity resulting from cloud-cloud collisions is the major factor in causing the rapid deceleration of the cloud phase immediately behind the shock front. We also proposed a complete galactic shock structure for both cloud and intercloud media.

CHAPTER V: CONCLUSIONS

This final chapter consists of some brief discussions and remarks of our results in the thesis.

CHAPTER II

DOUBLY PERIODIC SHOCK SOLUTIONS OF THE INTER-CLOUD MEDIUM

Similar calculations to those in Shu *et al*. are repeated with different parameters. The velocity of the cloud medium is assumed to be the same as the velocity of the intercloud medium. Our results are in good agreement with the results of Shu *et al*.

Moreover, we discuss the new models of the two-phase interstellar gas proposed by De Jong (1976). By adopting De Jong's equation of state of the interstellar gas, we carry out a detailed study of quasi-steady flows of interstellar gas including phase transition. The shock solutions are determined, and our results do agree again with that of Shu *et al*.

II-a Galactic shocks in an interstellar medium with two stable phases as proposed by Shu et al.

An important development was put forth by Shu et al. (1972). The shock formation problem was solved by treating the interstellar gas medium as two gaseous phases in rough pressure equilibrium with each other(Spitzer and Scott 1969, Field, Goldsmith, and Habing 1969). Phase transition occurs and the intercloud material condenses into cloud medium as pressure reaches its maximum value, P_{max}. Conversely, as pressure reaches its mimimum value, P_{min}, the cloud material evaporates into intercloud medium. They assume that both phases travel at the same speed all the time except in immediate postshock regions. The density and pressure relations of these two phases can be well represented by a polytropic relation.

$$P_{eq}(\rho, \xi_0) = K(\xi_0)\,\rho^{N+1/N}, \qquad (2\text{-}1)$$

where ρ is the density of the intercloud medium and P

is its pressure. ξ_0 is the ioniation rate, and $k(\xi_0) \propto \xi_0^{-1/N}$ is a constant for given ξ_c, $^{N+1}/_{N} = \gamma = 0.675$ in our calculations. We shall follow all the basic equations of Shu et al.(1972), as in the following forms.

$$\mathcal{V} = \mathcal{V}_0 + \mathcal{V}' , \qquad (2-2)$$

$$\vec{u} = \vec{u}_0 + \vec{u}' , \qquad (2-3)$$

$$\rho = \rho_0 + \rho' . \qquad (2-4)$$

Where $\mathcal{V}$ is the gravitational potential to be decomposed into a static axisymmetric potential $\mathcal{V}_0$ and a perturbed spiral potential $\mathcal{V}'$. The velocity $\vec{u}$, decomposed into $\vec{u}_0$ and $\vec{u}'$, $\vec{u}_0$ is the velocity which provides pure centrifugal force which balances against the radial galactic gravitational field, while $\vec{u}'$ is the corresponding velocity which overcomes the additional spiral gravitational field. Similarly, the density can be decomposed into ρ_0 which corresponds to the axisymmetric mass distributions and ρ' which corresponds to non-axisymmetric spiral mass distributions.

$$-\nabla \mathcal{U}_0(\varpi) = -\vec{e}_{\varpi}\,\varpi\,\Omega^2(\varpi),$$

$$\text{and}\quad \vec{U}_0 = \vec{e}_{\phi}\,\varpi\,(\Omega - \Omega_p), \qquad (2\text{-}5)$$

where ϖ is the radial distance from the galactic center, Ω_p is the pattern speed, and $\phi = \theta - \Omega_p t$ is the ϕ coordinate in the rotating cylindrical coordinates (ϖ, ϕ, Z).

$\vec{e}_{\phi}$ and $\vec{e}_{\varpi}$ are unit vectors along ϕ and ϖ directions. By introducing the orthogonal curvilinear coordinates (η, ξ, Z) (Roberts 1969), we obtain the following transformations

$$\begin{pmatrix}\eta\\ \xi\end{pmatrix} = \begin{pmatrix}\cos i & \sin i\\ -\sin i & \cos i\end{pmatrix}\begin{pmatrix}\ln\varpi\\ \phi\end{pmatrix}, \quad \begin{pmatrix}e_{\eta}\\ e_{\xi}\end{pmatrix} = \begin{pmatrix}\cos i & \sin i\\ -\sin i & \cos i\end{pmatrix}\begin{pmatrix}e_{\varpi}\\ e_{\phi}\end{pmatrix}. \qquad (2\text{-}6)$$

The spiral gravitational field at $Z = 0$ is

$$-\nabla\mathcal{U}' = \vec{e}_{\eta}\, g_1 = -\vec{e}_{\eta}\, F\,\varpi\,\Omega^2(\varpi)\sin\left(-\frac{2\eta}{\sin i}\right), \qquad (2\text{-}7)$$

where F is the fractional strength of the spiral gravitational field compared to the axisymmetric gravitational field F=0.05 in our calculations.

The Euler equations of the interstellar medium in a rotating frame with pattern speed Ω_p may be expressed in the following Vector forms.(Shu et al.1972, p 566).

$$\nabla\cdot(F_c\langle\rho_c\rangle h_c\vec{u}_c) = n_s h_c\langle\dot{M}\rangle, \tag{2-8}$$

$$\nabla\cdot[(1-F_c)\rho h\vec{u}] = -n_s h_c\langle\dot{M}\rangle, \tag{2-9}$$

$$\nabla\cdot(F_c\langle\rho_c\rangle h_c\vec{u}_c\vec{u}_c) - F_c\langle\rho_c\rangle h_c[-\nabla(\mathcal{V}-\tfrac{1}{2}\Omega_p^2\varpi^2)-2\vec{\Omega}_p\times\vec{u}]$$
$$-\nabla(F_c\langle\rho_c\rangle h_c c^2) - F_c\nabla(Ph) - Dh(u_c-u)+n_s h_c\langle\dot{M}\cdot\vec{v}'\rangle \tag{2-10}$$

$$\nabla\cdot[(1-F_c)\rho h\vec{u}\cdot\vec{u}] = (1-F_c)\rho h[-\nabla(\mathcal{V}-\tfrac{1}{2}\Omega_p^2\varpi^2-2\vec{\Omega}_p\times\vec{u}],$$
$$-(1-F_c)\nabla(Ph) - Dh(\vec{u}-\vec{u}_c) - n_s h_c\langle\dot{M}\cdot\vec{v}'\rangle. \tag{2-11}$$

Here we have to take few approximations similar to that of Shu et al. (1972) (1) $h = h_c$ =constant(2) $u = u_c$(3) $(1-F_c)h$ =constant (4) F_c ∇ p is negligible as compared to the other terms.We then integrate equations(2-8)–(2-11) along Z direction, adopting the logarithmic spiral coordinates (η , ξ) and apply the same asymptotic analysis of Roberts(1969).The equations become the following forms

$$\frac{d}{d\eta}(\rho u_\eta) = -\varepsilon\varpi, \tag{2-12}$$

$$\frac{d}{d\eta}(\sigma_c u_{c\eta}) = \varepsilon\varpi, \tag{2-13}$$

$$u_\eta \frac{du'_\eta}{d\eta} - 2\varpi\Omega u'_\xi = \frac{1}{\rho}\frac{dP}{d\eta} + g_1. \qquad (2\text{-}14)$$

$$u_\eta \frac{du'_\xi}{d\eta} = -\varpi\left(\frac{k^2}{2\Omega}\right) u'_\eta. \qquad (2\text{-}15)$$

$$u_{c\eta} \frac{du'_{c\eta}}{d\eta} - 2\varpi\Omega u'_{c\xi} = -\frac{c^2}{\sigma_c}\frac{d\sigma_c}{d\eta} + g_1. \qquad (2\text{-}16)$$

$$u_{c\eta} \frac{du_{c\xi}}{d\eta} = -\varpi\left(\frac{k^2}{2\Omega}\right) u'_{c\eta}. \qquad (2\text{-}17)$$

where ξ is the rate of phase transition per unit length and $\sigma_c = f_c \cdot \rho_c$ is the modified fractional volume of the cloud medium when the scale heights of both media are taken into account, which is defined as

$$f_c = \frac{F_c h_c}{(1-F_c)h} \qquad (2\text{-}18)$$

This definition is the result of dividing the equations of continuity(2-8) and (2-9) by$(1-F_c)$.Since we focus our present studies on the intercloud medium only, the equations(2-16) and (2-17) for cloud medium will not be considered in this chapter.

We assume that $\sin i \ll 1$ and ζ_0 is a constant along a streamline.If the phase transition does not occur along

the streamline, $\epsilon = 0$ then equations(2 − 12)−(2 − 15)become

$$\rho u_\eta = \text{constant}, \tag{2-19}$$

$$f_c \langle \rho_c \rangle u_\eta = \text{constant}. \tag{2-20}$$

$$\frac{\partial u'_\eta}{\partial \eta} = \frac{(2\varpi\Omega u'_\xi + \varpi g_1)}{u_\eta^2 - a^2}, \tag{2-21}$$

$$\frac{\partial u'_\xi}{\partial \eta} = \frac{-\varpi K^2 u'_\eta}{2\Omega u_\eta}, \tag{2-22}$$

where a is sonic speed of the intercloud medium, which is defined as

$$a^2 = \left(\frac{dP}{d\rho}\right)_{s_0}. \tag{2-23}$$

If the phase transition occurs along the streamline,then $\epsilon \neq 0$ and the pressure maintains at either P_{max} or P_{min}. Therefore $\frac{dP}{d\eta}$ is equal to zero. We add equations(2 − 12) and(2 − 13) to eliminate $\epsilon\varpi$ .Then the fluid equations become

$$(f_c \langle \rho_c \rangle + \rho) u_\eta = \text{constant}, \tag{2-24}$$

$$\frac{\partial u'_\eta}{\partial \eta} = \frac{2\varpi\Omega u'_\xi + \varpi g_1}{u_\eta}, \tag{2-25}$$

$$\frac{\partial u'_\xi}{\partial \eta} = \frac{-\varpi K^2 u'_\eta}{2\Omega u_\eta}. \tag{2-26}$$

The asymptotic equations (2 − 19)—(2 − 22) or (2− 24)—— (2—26) can be integrated numerically to determine the

steady large-scale flow of gas in the galaxy. The numerical integrations are carried out in sections(2-b) and (2-d) for the streamline which passes through the solar neighborhood. Doubly periodic shock solutions which contain phase transitions are also determined as shown in Figures(2-1) and (2-12).

In our calculations we adopt a model of two-phase interstellar medium similar to Shu et al. with a minor change of parameters, the pattern speed in our calculations Ω_p =12.5km $S^{-1}kpc^{-1}$ for the circular frequency Ω =25km $S^{-1}kpc^{-1}$. The pitch angle of the spiral arms is 7°. The sonic speed varies with respect to the local density of intercloud medium. In the calculations the sonic speed a is determined from the equation $a^2 = \left(\frac{\partial P}{\partial \rho}\right)_{S_0}$. Figure(2-2) shows the variations of local sonic speed which ranges from 6.793km/sec to 10.4593km/sec . The relative strength of the spiral gravitational force is F=0.05. The fractional volume occupied by the cloud medium is F_c.

II-b Results:COMFIRMATION OF THE RESULTS OF SHU ET AL(1972)

Our results are presented in graphical form as shown in Figures(2-1)——(2-8). The same lables SP, A, B, Sh, 1, and 2 as in Shu et al. are adopted. SP is the sonic point, and A is the location where the phase transition starts. B is the location where the phase transition ceases, and Sh is the location of shock. Locations 1 and 2 correspond to the preshock and postshock locations. The horizontal axes as shown in Figures(2-1)—(2-8) correspond to the phase angle $\phi = \theta - \Omega_p t$.

Figure(2-1): The STS solution(streamtube band through two periodically located shocks) for the streamline passes through the solar neighborhood. The numerical integrations start at SP(sonic point). First we integrate forward in η along the supersonic branch. The flow is decompressional, and the pressure decreases steadily until the pressure P becomes P_{min} at location A where the phase transition starts. There is a steady net flow of mass evaporated from the cloud medium into the intercloud

medium; meanwhile, the pressure remains unchanged. The velocity increases steadily along the vertical direction and reaches its maximum at location B. Thereafter the flow becomes compressional, and the phase transition ceases. The forward integrations end at regions beyond the preshock location 1. The subsonic integrations are performed backwards from the sonic point(SP) to the regions beyond the postshock location 2. The flow along the subsonic branch is compressional and the pressure increases steadily until location 2, where the pressure $P=P_{max}$. At each step of the supersonic intergrations, we use the jump conditions to determine the downstream locations of the shock. The curve begining at SP and passing through A', B', and point 2 is constructed by the corresponding downstream locations of STS solution. The postshock location 2 is the intersection of the curve of backward integrations and the curve passing through SP, A',and B'. The gas flow reaches its preshock conditions at location 1, then undergoes a violent shock via the jump conditions,

and reaches its downstream location 2. The amount of mass lost from the cloud medium to the intercloud medium between locations A and B is fully reclaimed by the cloud medium at location 2.

Figure(2-2): The variation of sonic speed along a streamline which passes through the solar neighborhood. The maximum sonic speed is in the region between location A and location B, where the pressure $P=P_{min}$ and the maximum sonic speed $a_{max}=10.4593$km/sec. The minimum sonic speed is located at postshock location 2, where the pressure $P=P_{max}$ and the minimum sonic speed $a_{min}=6.793$km/sec. The sonic speed at sonic point $a_{sp}=8.38868$km/sec.

Figure(2-3): The variation of the tangential velocity of the interstellar gas along the entire streamline which passes through the solar neighborhood.

Figure(2-4): The variation of the normal velocity of

the interstellar gas along the entire streamline which passes through the solar neighborhood.

Figure(2-5): The variation of the pressure of the interstellar gas along the entire streamline which passes through the solar neighborhood. From location A to location B, the phase transition occurs, and there is transformation of cloud material into intercloud material. Meanwhile the pressure remains constant at $P_{min}=4.167\times10^{-14}$dynes/cm^2. At postshock location 2, the pressure $P=P_{max}=2.087\times10^{-13}$dynes/cm^2 and the phase transition occurs again. There the cloud medium fully reclaims its lost mass from the intercloud medium.

Figure(2-6): The variation of the number density of the intercloud medium along the entire streamline. Between location A and location B, the number density n remains unchanged at $n_{min}=0.016338/cm^3$. At location 2 the number density $n=n_{max}=0.17774/cm^3$. At the sonic point, $n=n_{sp}=0.052625/cm^3$.

Figure(2-7): The variation of the local fraction of volume occupied by the cloud medium F_c along the entire streamline. Starting at sonic point SP, the flow is decompressional. The value of F_c increases steadily until location A, where F_c reaches its maximum value $F_{cmax}=0.15449$. This value means that 15.449% of the local volume is occupied by the clouds and that 93.7234% of the total mass of the local interstellar material is concentrated in the cloud medium. The intercloud medium retains only 6.2766% of the total mass of the local interstellar material. Between locations A and B, the pressure remains unchanged at $P=P_{min}$. Meanwhile the cloud medium steadily loses its mass to the intercloud medium due to phase transition. At location B, $F_c=0.12219$. Only 12.219% of the local volume is occupied by clouds and 87.781% of the local volume is occupied by the intercloud medium. Equivalently, 74.128237% of the total mass of the local interstellar material is in the cloud medium, and 25.871763% of the total mass of the interstellar material

is in the intercloud medium. Thereafter the gas flow becomes compressional until the postshock location 2. There $F_c=F_{cmin}=0.066068$, and $P=P_{max}$. The cloud medium occupies only 6.6068% of the local volume, and the phase transition occurs once again. At location 2 the cloud medium fully reclaims its lost mass from the intercloud medium. The cloud medium once again constitutes 93.7234% of the total mass of the local interstellar material immediately after the galactic shock.

Figure(2-8): The variation of the radius of the entire streamline which passes through the solar neighborhood. The nonclosure of the streamline(see Shu et al. 1972) exists between location 1 and 2.

Despite the fact that an entirely different numerical scheme is used, the above results do show a good agreement with that of Shu et al.(1972). Since we use the same model of two-phase interstellar gas with a minor change in parameters, we have doubly checked the complicated,but important calculations of Shu et al, as well as our numerical scheme to be used for the case of De Jong's model.

Figure 2-1: The procedure used to locate the galactic shock(STS solution) for Shu's model. Explanations are presented in section II-b.

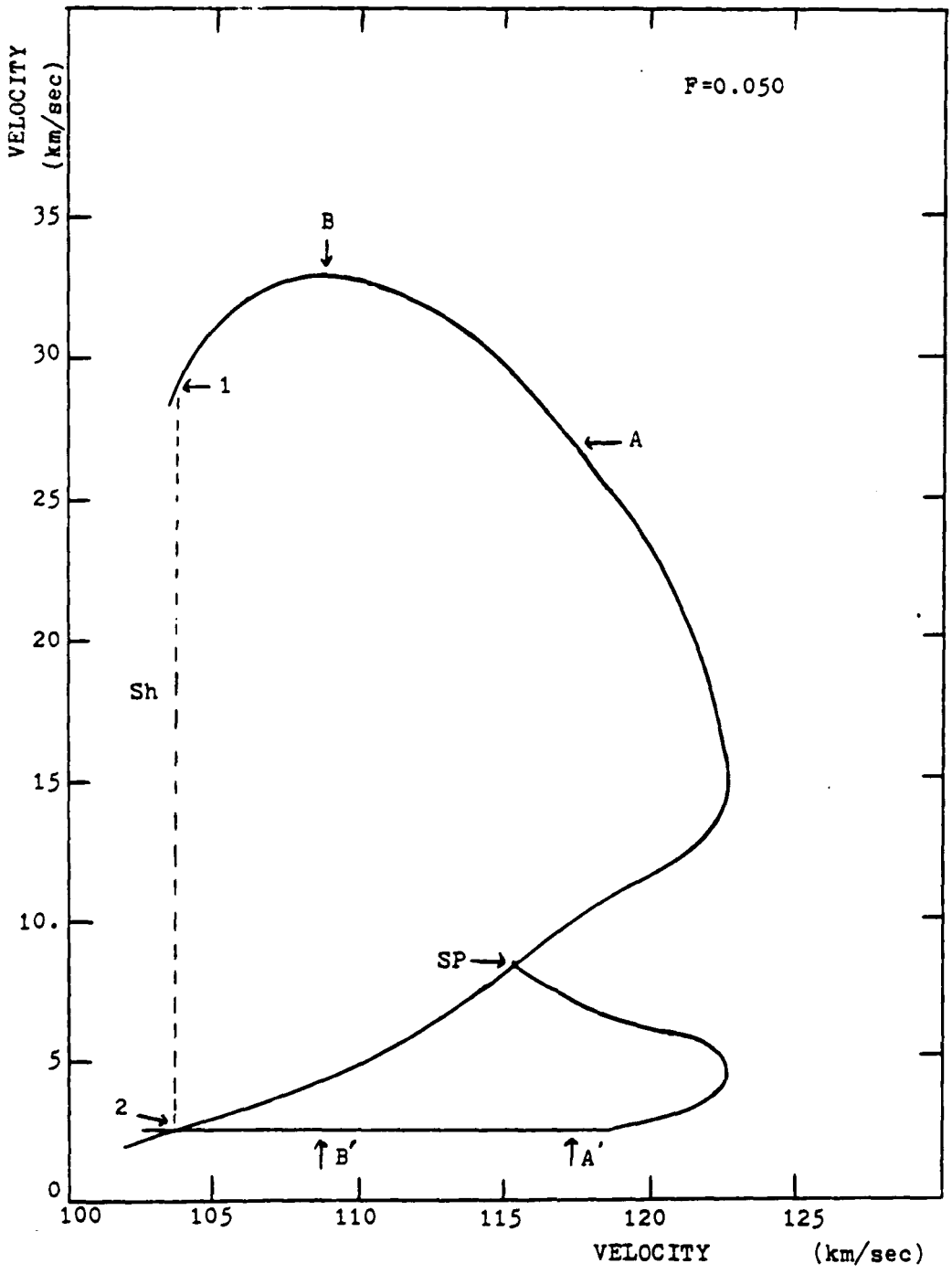
VELOCITY (km/sec)
F=0.050
B
1
A
Sh
SP
2
B'
A'
35
30
25
20
15
10.
5
0
100
105
110
115
120
125
VELOCITY (km/sec)

Figure 2-1

Figure 2-2: The variation of local sonic speed along a streamline which passes through the solar neighborhood.(Shu's model)

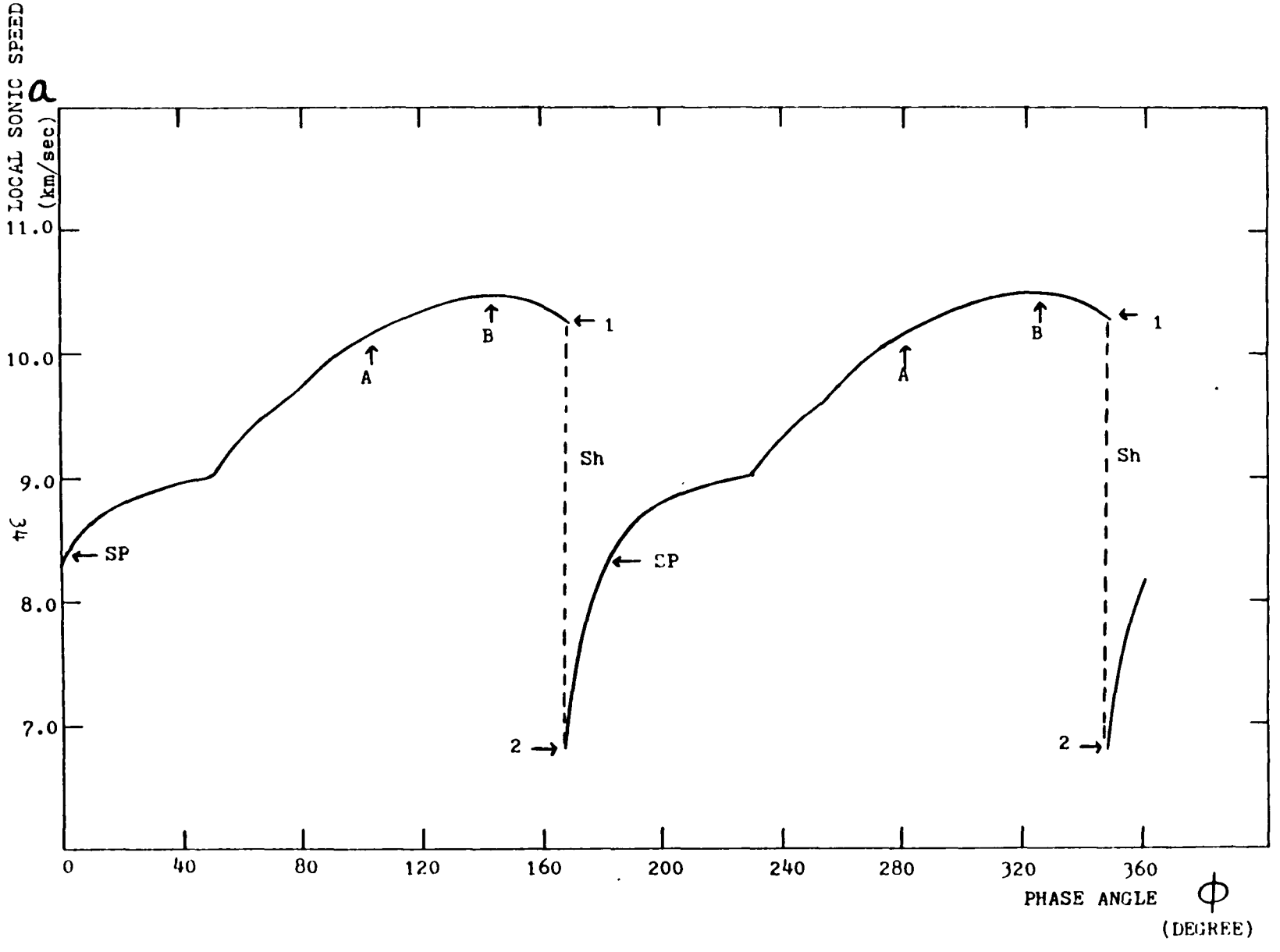
LOCAL SONIC SPEED
a
(km/sec)
11.0
10.0
9.0
8.0
7.0
SP
A
B
1
Sh
2
SP
A
B
1
Sh
2
0
40
80
120
160
200
240
280
320
360
PHASE ANGLE
(DEGREE)

Figure 2-2

Figure 2-3: The variation of the tangential velocity of the interstellar gas along the entire streamline which passes through solar neighborhood.(Shu's model)

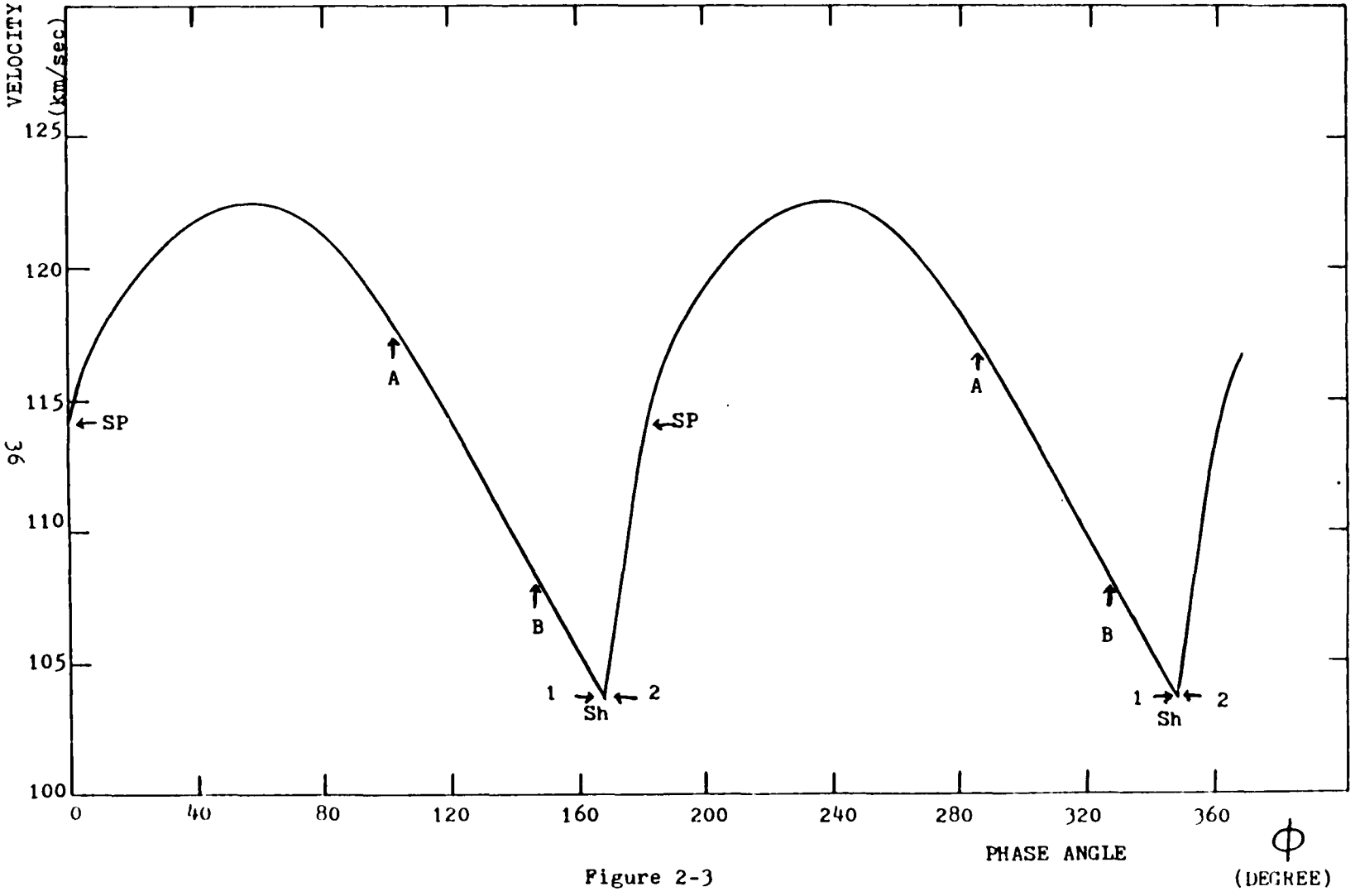
VELOCITY (km/sec)
125
120
115
110
105
100
SP
A
B
1
Sh
2
SP
A
B
1
Sh
2
0
40
80
120
160
200
240
280
320
360
PHASE ANGLE
Φ
(DEGREE)

Figure 2-3

Figure 2-4: The variation of the normal velocity of the interstellar gas along the entire streamline which passes through the solar neighborhood.(Shu's model)

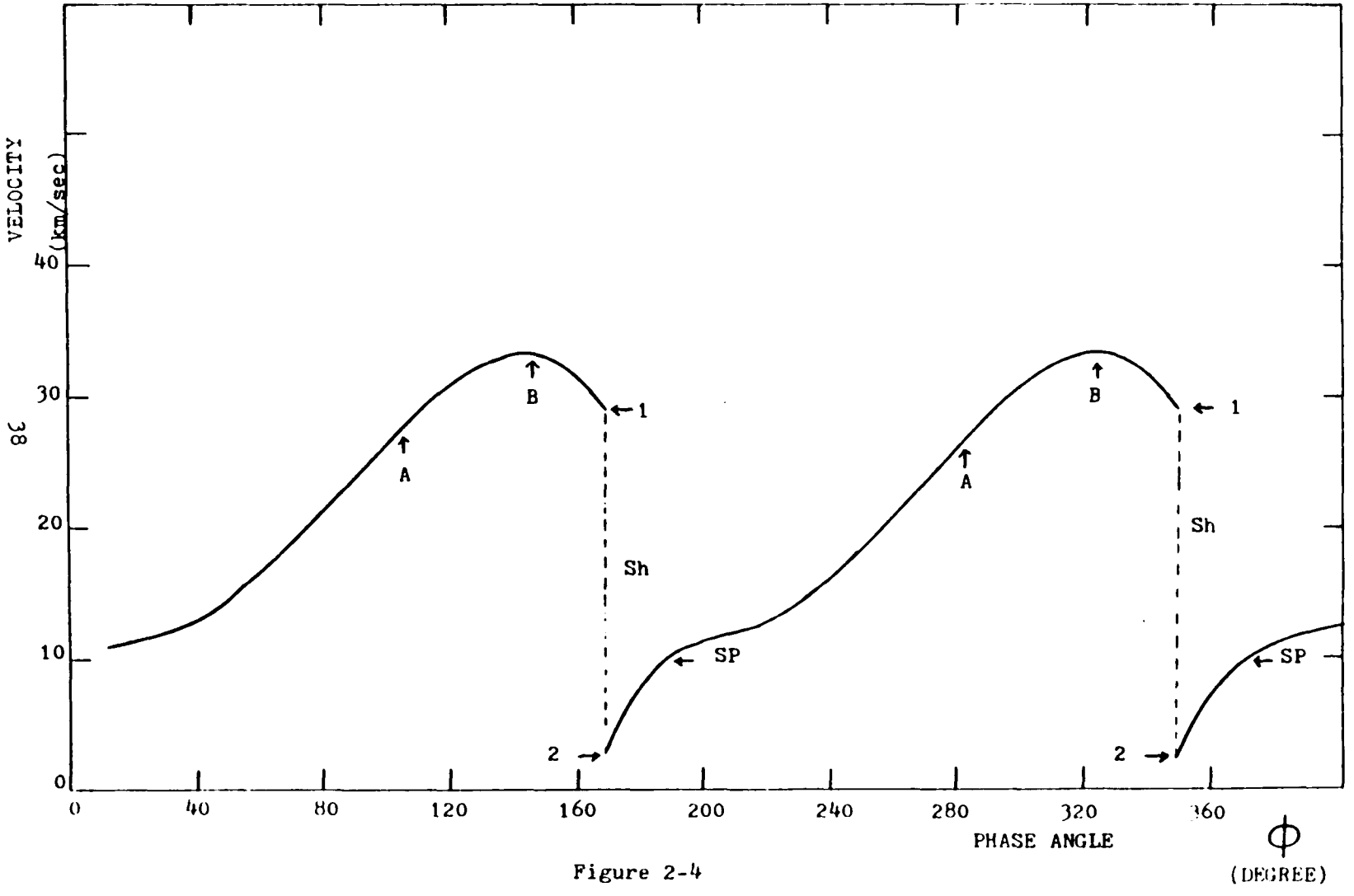
VELOCITY
(km/sec)
40
30
20
10
0
A
B
1
Sh
SP
2
A
B
1
Sh
SP
2
0
40
80
120
160
200
240
280
320
360
PHASE ANGLE
Φ
(DEGREE)

Figure 2-4

Figure 2-5: The variation of the pressure of the interstellar gas along the entire streamline which passes through the solar neighborhood.(Shu's model)

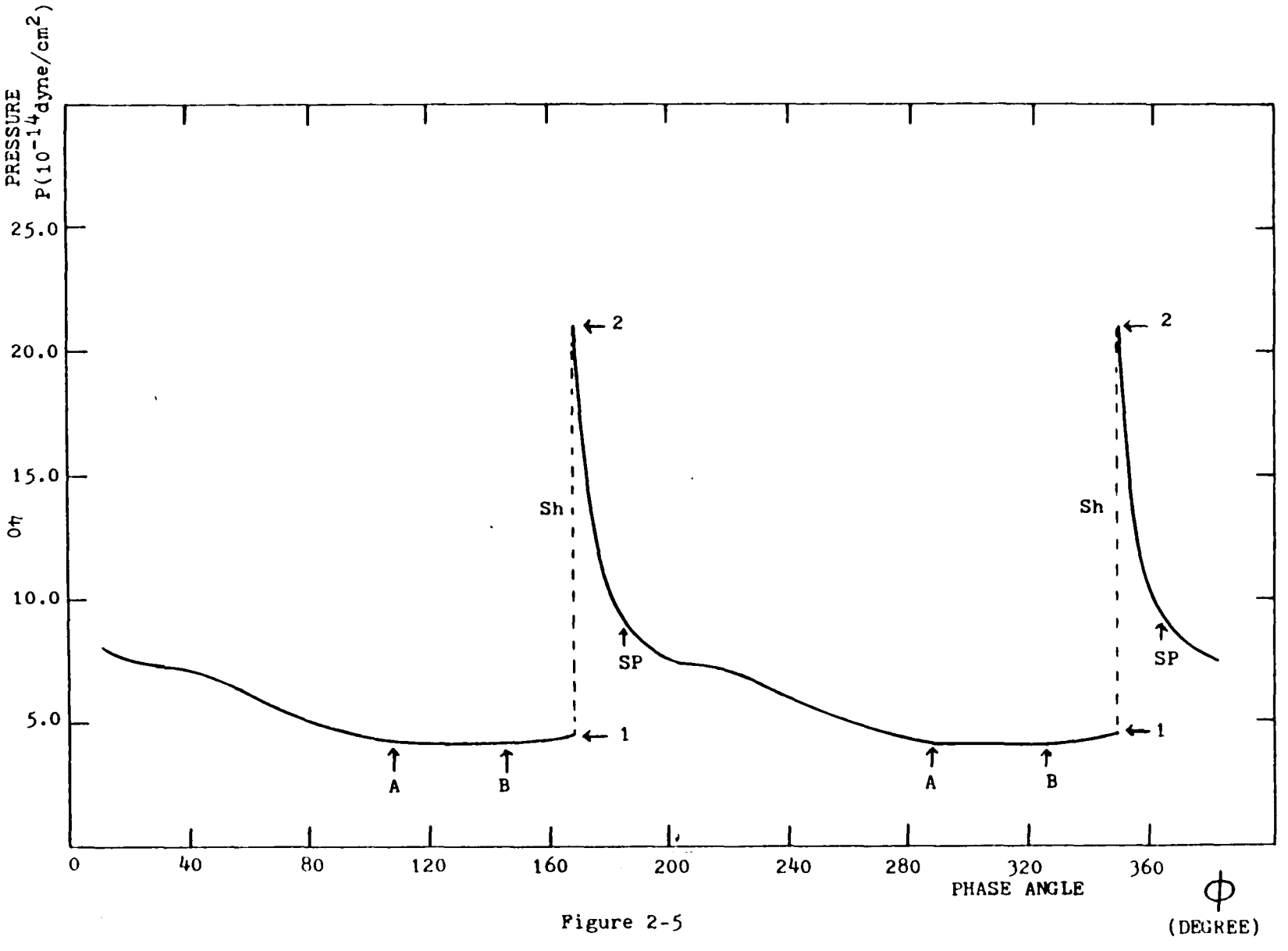
PRESSURE
P(10^{-14}dyne/cm^2)
25.0
20.0
15.0
10.0
5.0
0η
Sh
Sh
2
2
1
1
SP
SP
A
B
A
B
0
40
80
120
160
200
240
280
320
360
PHASE ANGLE
Φ
(DEGREE)

Figure 2-5

Figure 2-6: The variation of the number density of the intercloud medium along the entire streamline. (Shu's model)

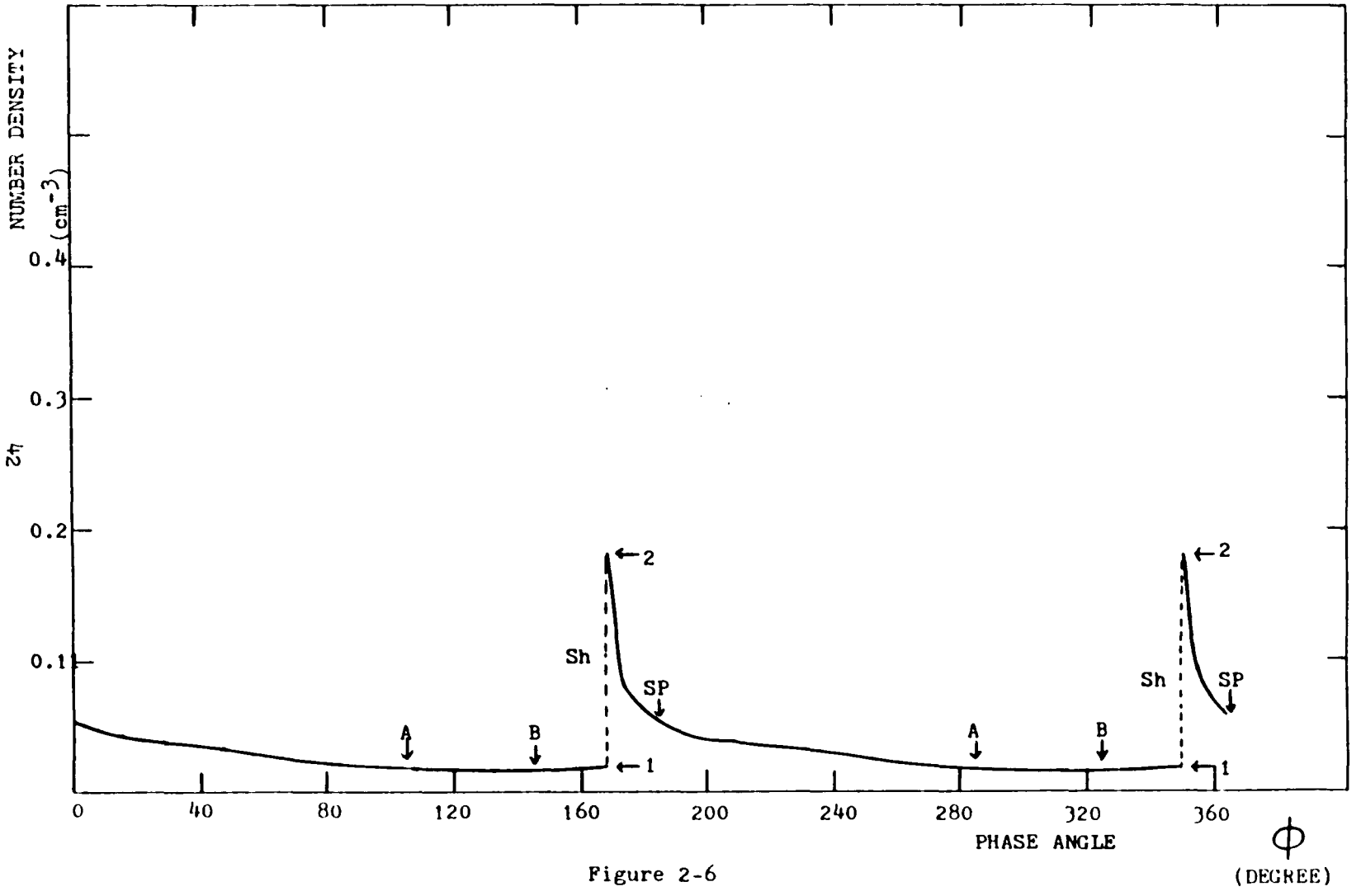
NUMBER DENSITY
(cm⁻³)
0.4
0.3
0.2
0.1
42
Sh
SP
A
B
1
2
0
40
80
120
160
200
240
280
320
360
PHASE ANGLE
Φ
(DEGREE)

Figure 2-6

Figure 2-7: The variation of the local fraction of volume occupied by the cloud medium F_c along the entire streamline.(Shu's model)

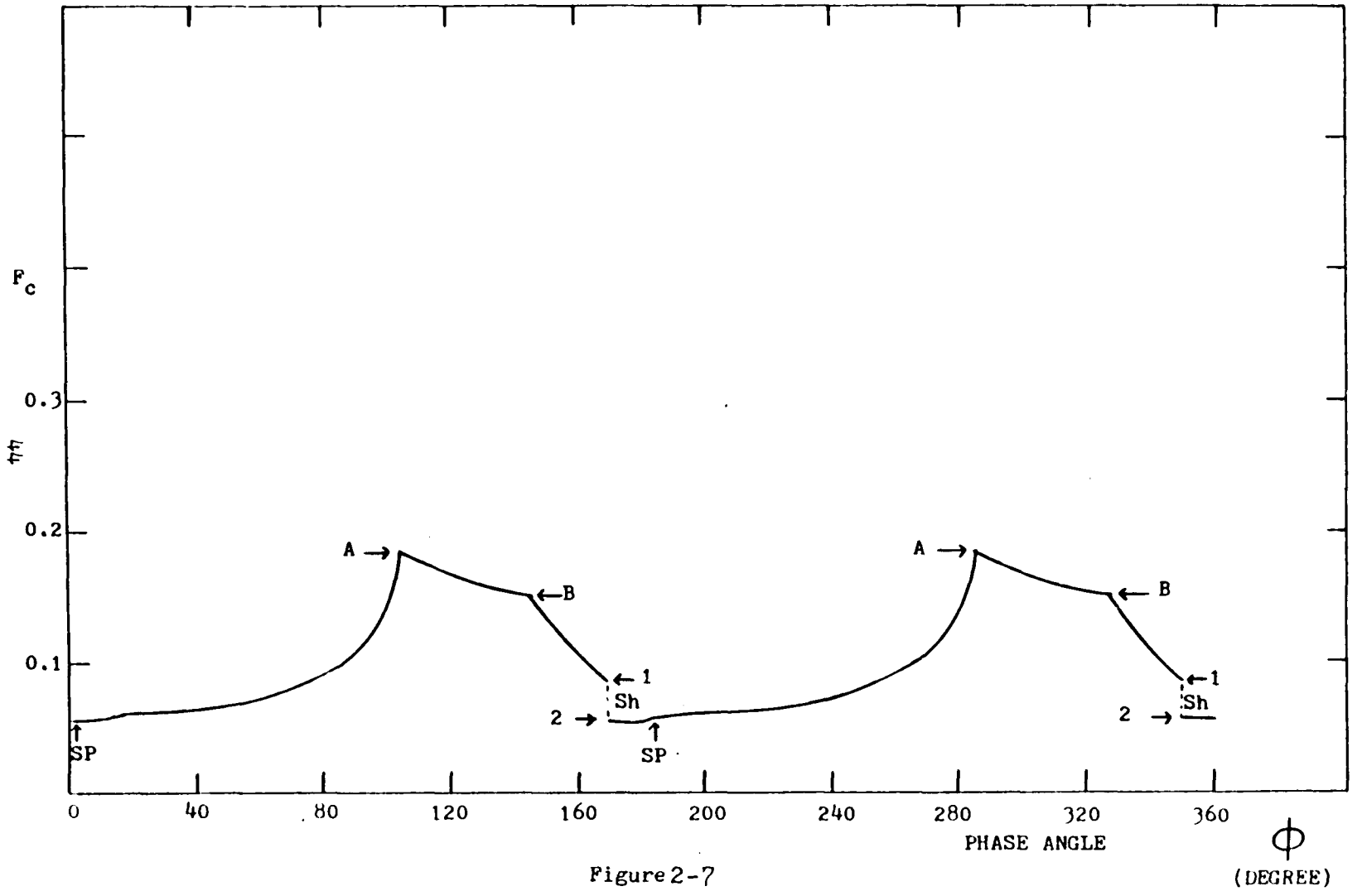
F_c
0.3
0.2
0.1
A
B
1
Sh
2
SP
SP
A
B
1
Sh
2
0
40
80
120
160
200
240
280
320
360
PHASE ANGLE
Φ
(DEGREE)

Figure 2-7

Figure 2-8: The variation of the radius of the entire streamline which passes through the solar neighborhood. (Shu's model)

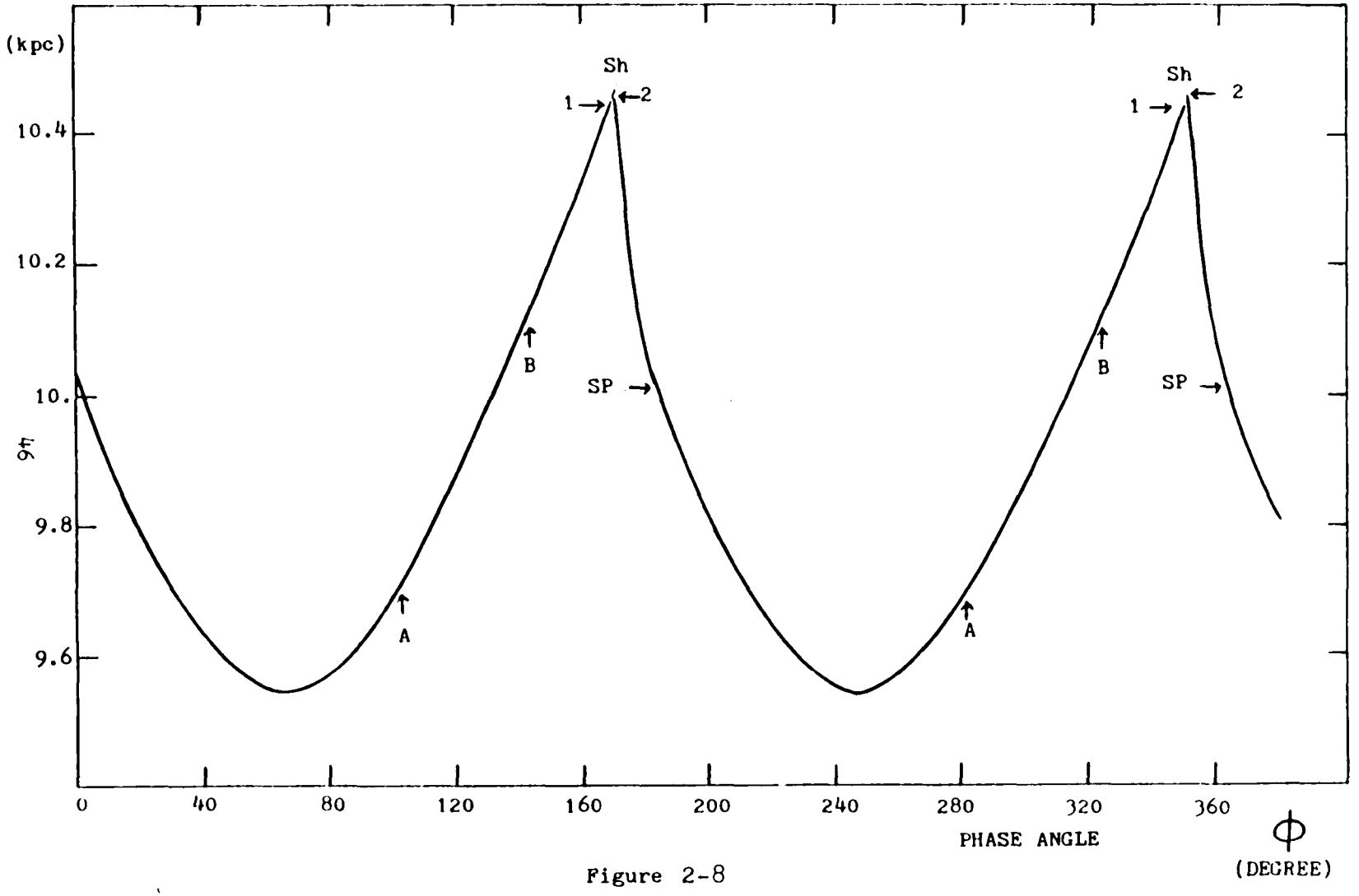
(kpc)
10.4
10.2
10.
9.8
9.6
r
Sh
1
2
B
SP
A
0
40
80
120
160
200
240
280
320
360
PHASE ANGLE
Φ
(DEGREE)

Figure 2-8

II-c Doubly shock solutions for the two-phase model of interstellar gas proposed by De Jong

The two-phase model of interstellar gas proposed by Spitzer and Scott (1969) and Field, Goldsmith, and Habing (1969) has largely broadened our understanding of the physical properties of the interstellar gas.In their models the only heating source for the interstellar gas is low-energy cosmic rays. In order to obtain agreement with the observations, a very high flux of low-energy cosmic rays must be postulated. The primary cosmic ray ionization rate of atomic hydrogen ζ_0 is assumed to be 1.2×10^{-15} S^{-1} by Shu et al. (1972) which is at least one order of magnitude higher than the upper limit—— $\zeta_0 \leq 10^{-16} S^{-1}$ derived from the observational results of the OH and HD densities in interstellar clouds by Black and Dalgarno (1973) and O'Donnell and Watson (1974). Unless there are other heating sources that exist in the galactic plane,

heating interstellar gas by low-energy cosmic rays alone is not enough to obtain a persuasive result for a two-phase interstellar gas in thermal and ionization balance. Watson(1972) suggested another effective source—— the photoelectrons from dust grains produced by ultraviolet photons of the interstellar radiation field of wavelength between 1200A and 912A.

De Jong(1976) calculated various models of the equation of state of the interstellar gas in thermal and ionization equilibrium. In addition to the insufficient low-energy cosmic ray heating source, he introduced the heating source of photoelectrons from dust grains suggested by Watson(1972). The intensity of the flux of the photoelectrons from dust grains depends on the photoelectric emission efficiency of dust grain Y, while the intensity of the flux of low-energy cosmic rays is proportional to the cosmic ray ionization rate of atomic hydrogen ζ_0. The H and He atoms are assumed to be ionized by low-energy

cosmic rays, while the atoms of heavy elements such as C, Mg, Si, S and Fe are ionized by the photons between 1200Å and 912Å. The equilibrium calculations are subject to the following conditions as stated by Spitzer and Scott(1969), (1) the ionization and recombination cross sections of H and He are equal; (2) H and He have the same degree of ionization;(3) there is no secondary ionization of He. The ionization equilibrium of H and He can be written as the equation

$$\zeta_0 [(1+\chi_{He})(1+\phi) + 2\chi_{He}] n(H) = \alpha_H(T) n(H^+)(1+\chi_{He}) n(e), \qquad (2\text{-}27)$$

where χ_{He} is the abundance of He relative to H. The $(1+\phi)$ factor accounts for the ionization by secondary electrons. $2\chi_{He}$ accounts for the ionization of H atoms by He recombination photons. $\alpha_H(T)$ is the hydrogen recombination coefficient.

The ionization equilibrium for heavy elements can be written as a series of equations

$$\beta_A(\chi) n(A) = \alpha_A(T) n(A^+) n(e), \qquad (2\text{-}28)$$

where β_A is the photoionization rate of atom A and α_A is its recombination coefficent. The heating and cooling equilibrium can be represented by the following funtional relations as stated by De Jong(1976)

$$\Gamma[\xi_0, Y, \chi, n, n(H), n(C), n(e), T] \quad (2\text{-}29)$$
$$= \Lambda[n(H), n(C^+), n(N), n(O), n(Si^+), n(S^+), n(Fe^+), n(e), T],$$

where Γ is the heating rate and Λ is the cooling rate. By solving simultaneous equations(2-27), (2-28), and (2-29), we find that the pressure of the interstellar gas can be represented by

$$P = KT \Sigma n_i , \quad (2\text{-}30)$$

where Σn_i is the sum of atoms, ions, and electrons. The equation of state for the interstellar gas can be well represented by the following polytropic relation for various values of ξ_0 and Y.

$$P_{eq}(\rho, \xi_0) = K(\xi_0)\rho^{\gamma} . \quad (2\text{-}31)$$

The equations of state determined by De Jong(1976) are presented in the following graphical forms.

Figure(2-9): <u>The various equations of state for the interstellar gas by De Jong(1976).</u> The cosmic ray ion-

ization rate is assumed to be $\zeta_0 = 10^{-15} s^{-1}$, while the photoelectric emission efficiency of dust grain Y is equal to 0, 0.01, 0.1 and 1.0 respectively as marked on each curve.

Figure(2-10): The same as Figure(2-9), except $\zeta_0 = 10^{-16} s^{-1}$ Between the tick mark on the left and the dot on the right is the region which is stable against thermal instability.

Figure(2-11): The same results as Figure(2-9), except ζ_0 is equal to $10^{-17} s^{-1}$.

Among these models of equations of state for the interstellar gas, the one that best fits the observations is when Y=0.1 and $\zeta_0 = 10^{-16} s^{-1}$, in fig.(2—10) which corresponds to $K(\zeta_0) = 8600$ and $\gamma = 0.675$ of equation(2-31) in our calculations. Based on the equation of state(equation 2-31) as well as equations(2-12)——(2-22), a set

of STS solutions can be obtained through the similar integrations as done in section II-a. In our calculations the pattern speed Ω_p =12.5km $s^{-1}kpc^{-1}$ for ϖ =10kpc; the circular frequency Ω =25km $s^{-1}kpc^{-1}$; and the pitch angle i =5.65°. The relative strength of the spiral gravitational force F =0.06. The fractional volume occupied by the cloud medium is F_c. The random velocity of cloud motions C =10km/sec. The results of our calculations are presented in the following section.

II-d. Results

Figure(2-12): The STS solution for the streamline passing through the solar neighborhood. The numerical integrations start at SP(sonic point). First, we integrate forward in η along the supersonic branch. The flow is decompressional, and the pressure decreases steadily until the pressure P becomes P_{min} at location A where the phase transition starts. There is a steady net flow of mass evaporated from the cloud medium into the intercloud medium; meanwhile the pressure remains unchanged. The velocity increases steadily along the vertical direction and reaches its maximum at location B. Thereafter the flow becomes compressional, and the phase transition ceases. The forward integrations end at regions beyond the preshock location 1. The subsonic integrations are performed backwards from the sonic point(SP) to the regions beyond the postshock location point 2. The flow along the subsonic branch is compressional, and the pressure increases steadily until location 2, where the pres-

sure $P=P_{max}$. At each step of the supersonic intergrations, we use the jump conditions, to determine the downstream locations of the shock. The curve begining at SP and passing through A', B', and point 2 is constructed by the corresponding downstream locations of STS solution. The postshock location 2 is the intersection of the curve of backward integrations and the curve passing through SP, A', and B'. The gas flow reaches its preshock conditions at location 1, then undergoes a violent shock and reaches its downstream location 2, via the jump conditions. The amount of mass that is lost from the cloud medium to the intercloud medium between location A and location B is fully reclaimed by the cloud medium at location 2.

Figure(2-13): The variation of sonic speed along a streamline which passes through the solar neighborhood. The maximum sonic speed is in the regions between location A and location B, where the pressure $P=P_{min}$ and the maximum sonic speed a_{max}=7.14km/sec. The minimum sonic speed is located at postshock location 2, where

the pressure $P=P_{max}$ and the minimum sonic speed $a_{min}=4.425$km/sec. The sonic speed at sonic point a_{sp} is equal to 7.14km/sec.

Figure(2-14): The variation of the tangential velocity of the interstellar gas along the entire streamline which passes through the solar neighborhood.

Figure(2-15): The variation of the vertical speed of the interstellar gas along the entire streamline which passes through the solar neighborhood.

Figure(2-16): The variation of the pressure of the interstellar gas along the entire streamline which passes through the solar neighborhood. From location A to location B, the phase transition occurs, and there is transformation of cloud material into intercloud material. meanwhile, the pressure remains constant at $P_{min}=2.14124\times10^{-13}$dynes/cm^2 . At postshock location 2,

the pressure $P=P_{max}=6.244x10^{-13}$dynes/cm^2 and the phase transition occurs again. There the cloud medium fully reclaims its lost mass from the intercloud medium.

Figure(2-17) : The variation of the number density of the intercloud medium along the entire streamline. Between location A and location B, the number density n remains unchanged at $n_{min}=0.14701/cm^3$. At location 2 the number density $n=n_{max}=0.7499/cm^3$. At the sonic point $n=n_{sp}=0.31273/cm^3$.

Figure(2-18) : The variation of the local fraction of volume occupied by the cloud medium F_c along the entire streamline. Starting at sonic point SP, the flow is decompressional. The value of F_c increases steadily until location A, where F_c reaches its maximum value $F_{cmax}=0.14545$. This value means that 14.545% of the local volume is occupied by the clouds and that 86.255% of the total mass of the local interstellar material is concentrated in the cloud medium. The intercloud medium retains only 13.745%

of the total mass of the local interstellar material. Between locations A and B, the pressure remains unchanged at $P=P_{min}$. Meanwhile the cloud medium steadily loses its mass to the intercloud medium due to phase transition. At location B, $F_c=0.04774$. Only 4.774% of the local volume is occupied by clouds and 95.226% of the local volume is occupied by the intercloud medium. Equivalently, 64.89% of the total mass of the local interstellar material is in the cloud medium, and 35.11% of the total mass of the interstellar material is in the intercloud medium. Thereafter the gas flow becomes compressional until the post-shock location 2. There $F_c=F_{cmin}=0.0330363$ and $P=P_{max}$. The cloud medium occupies only 3.30363% of the local volume. Then the phase transition occurs once again. At location 2 the cloud medium fully reclaims its lost mass from the intercloud medium. The cloud medium once again constitutes 86.255% of the total mass of the local interstellar material immediately after the galactic shock.

Figure(2-19): The variation of the radius of the entire streamline which passes through the solar neighborhood. The nonclosure of the streamline(see Shu et al. 1972) exists between location 1 and location 2.

The above results bears a considerable resemblance to that of Shu et al.(1972). However,there are some differences between them as listed in the following.

(1) This model fits better to the observations due to a smaller value of the ionization rate.

(2) The average density of the interstellar gas in this model is about five times higher than Shu's model for the intercloud medium, while it is three times higher than Shu's model for the cloud medium.

(3) The average pressure is about four times higher than Shu's model. On the contrary, the ratio of the maximum pressure to the minimum pressure—— $\frac{P_{max}}{P_{min}}$ is only about three times in this model while it is five times in Shu's model. Therefore the gas flows reach their maximum pressure and undergo phase transition shortly after the sonic point.

Phase transitions exist along most part of the streamline, which result in a greater mass, momentum, and energy transport between the cloud and the intercloud phases.

(4) The sonic speed is considerably lower than that of Shu's model(8 km s^{-1}), especially in the shock layer, which results in a longer dynamic timescale of the various physical processes such as slower propagation of forced pressure disturbances in the intercloud medium, and longer sound travel time through the cloud medium.

(5) The shock strength—— $\frac{P_{post\text{-}shock}}{P_{pre\text{-}shock}}$ equals 3 in this case, which is weaker than Shu's model(shock strength 5).

(6) Although the maximum density of the cloud medium in this model is 2.5 times higher than Shu's model. However, due to higher kinetic energy of the cloud medium in this model the critical mass of cloud for gravitational collapse is not smaller than Shu's model.

Figure 2-9.——2-11: Models of two-phase interstellar gas which proposed by De Jong(1976).

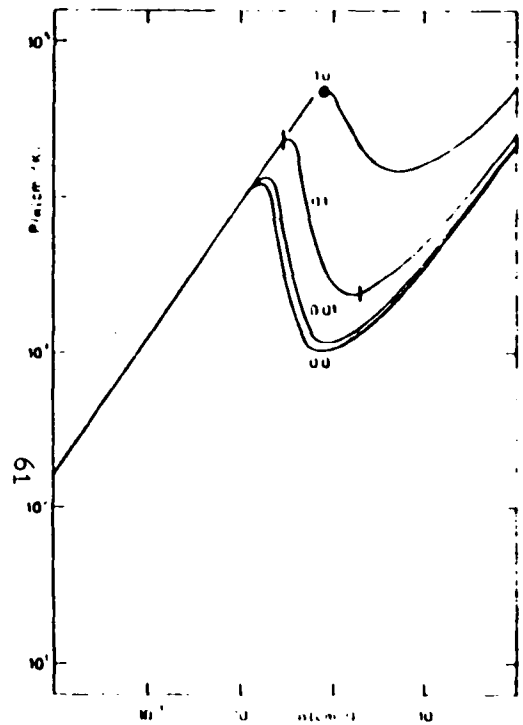

Figure 2-9

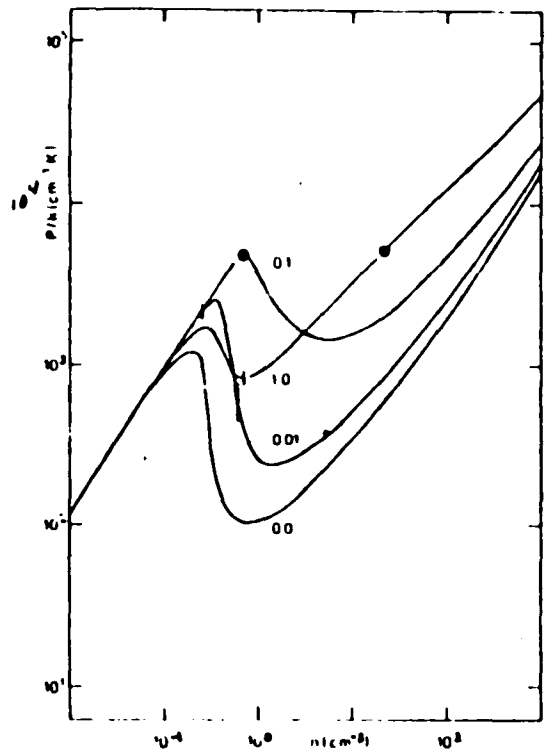

Figure 2-10

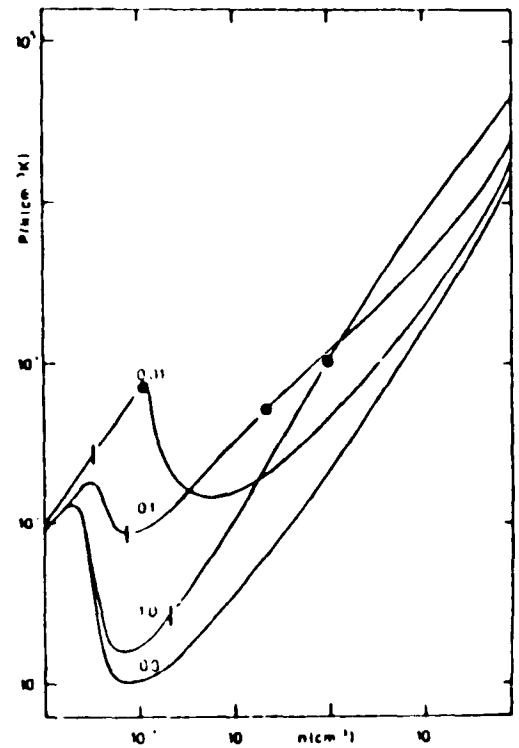

Figure 2-11

Figure 2-12: The procedure used to locate the galactic shocks(STS solution) for De Jong's model. Explanations are presented in section II-d.

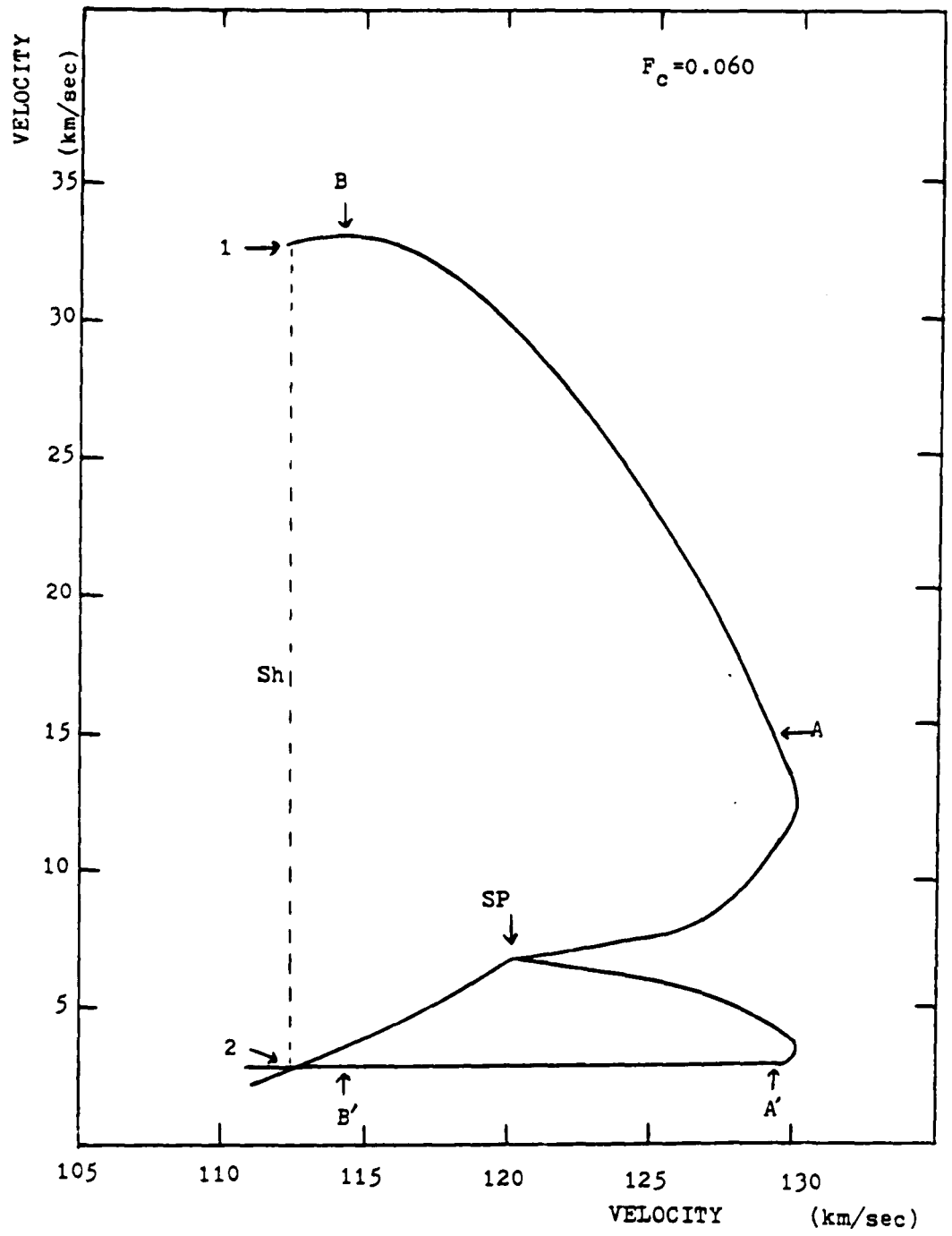
VELOCITY (km/sec)
F_c=0.060
35
30
25
20
15
10
5
B
1
Sh
A
SP
2
B′
A′
105
110
115
120
125
130
VELOCITY (km/sec)

Figure 2-12

Figure 2-13: The variation of local sonic speed along a streamline which passes through the solar neighborhood. (De Jong's model)

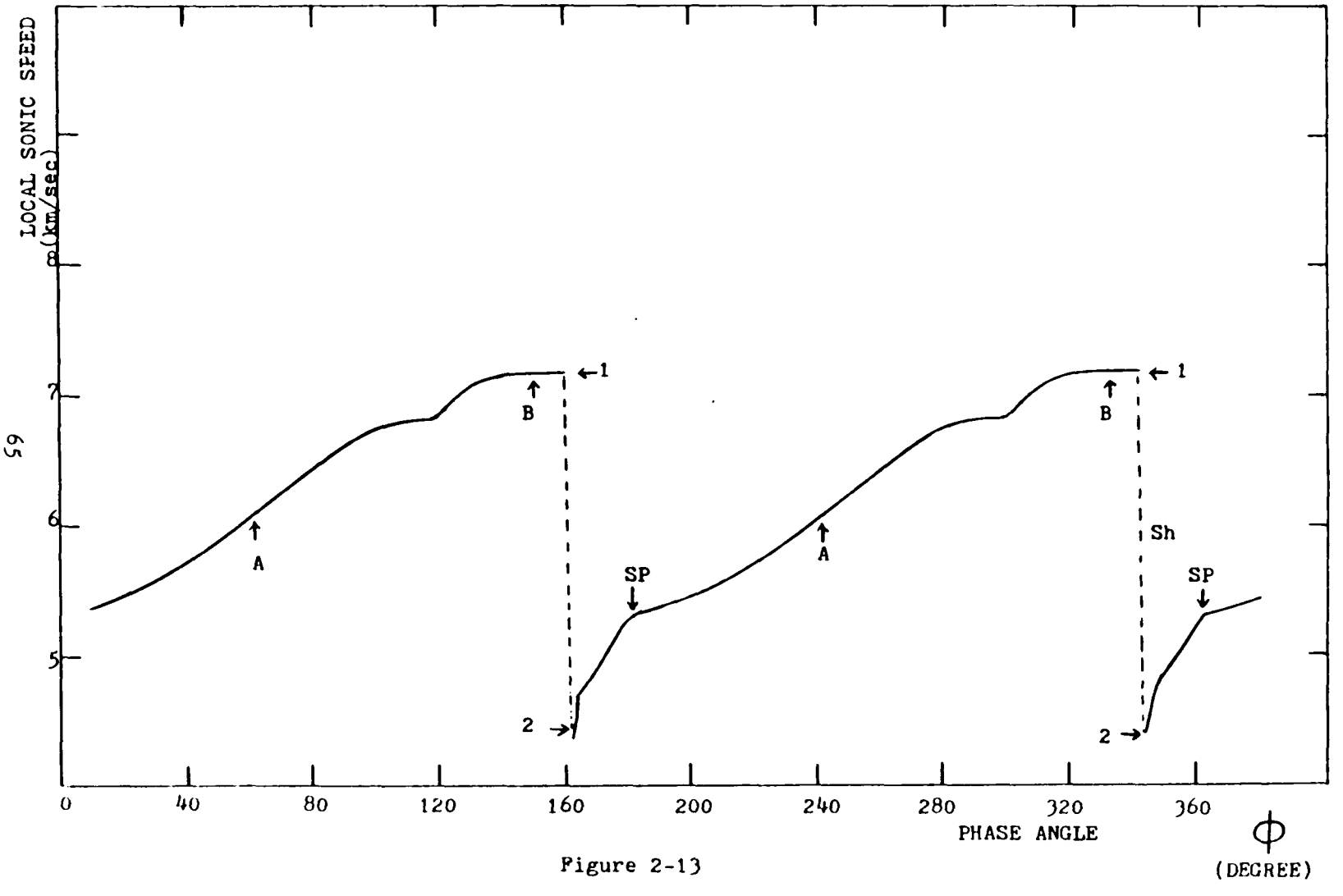
LOCAL SONIC SPEED
a(km/sec)
7
6
5
A
B
1
2
SP
Sh
0
40
80
120
160
200
240
280
320
360
PHASE ANGLE
Φ
(DEGREE)

Figure 2-13

Figure 2-14: The variation of the tangential velocity of the interstellar gas along the entire streamline which passes through solar neighborhood.(De Jong's model)

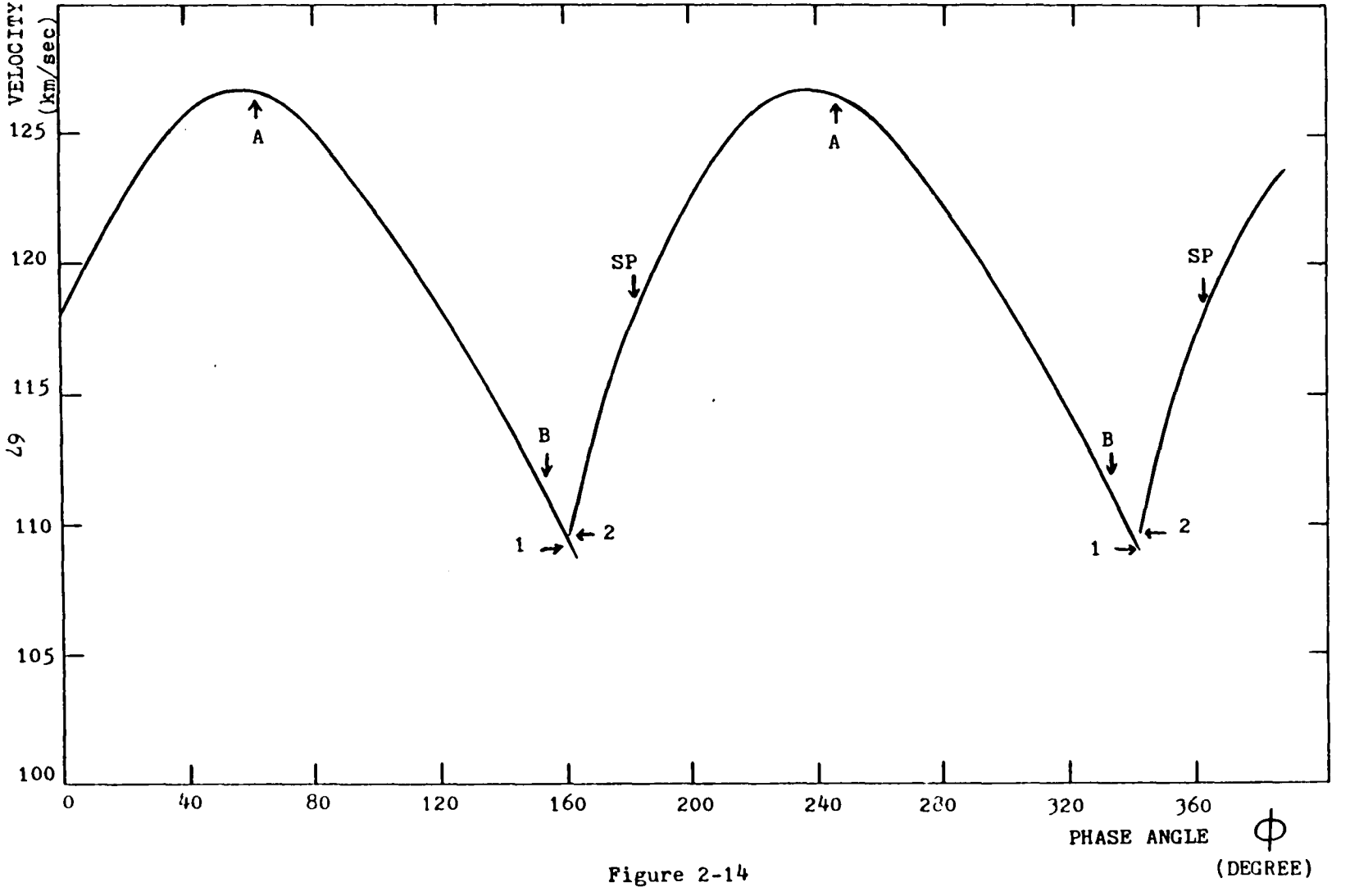
VELOCITY (km/sec)
125
120
115
110
105
100
A
A
SP
SP
B
B
1
2
1
2
0
40
80
120
160
200
240
280
320
360
PHASE ANGLE Φ
(DEGREE)

Figure 2-14

Figure 2-15: The variation of the normal velocity of the interstellar gas along the entire streamline which passes through the solar neighborhood.(De Jong's model)

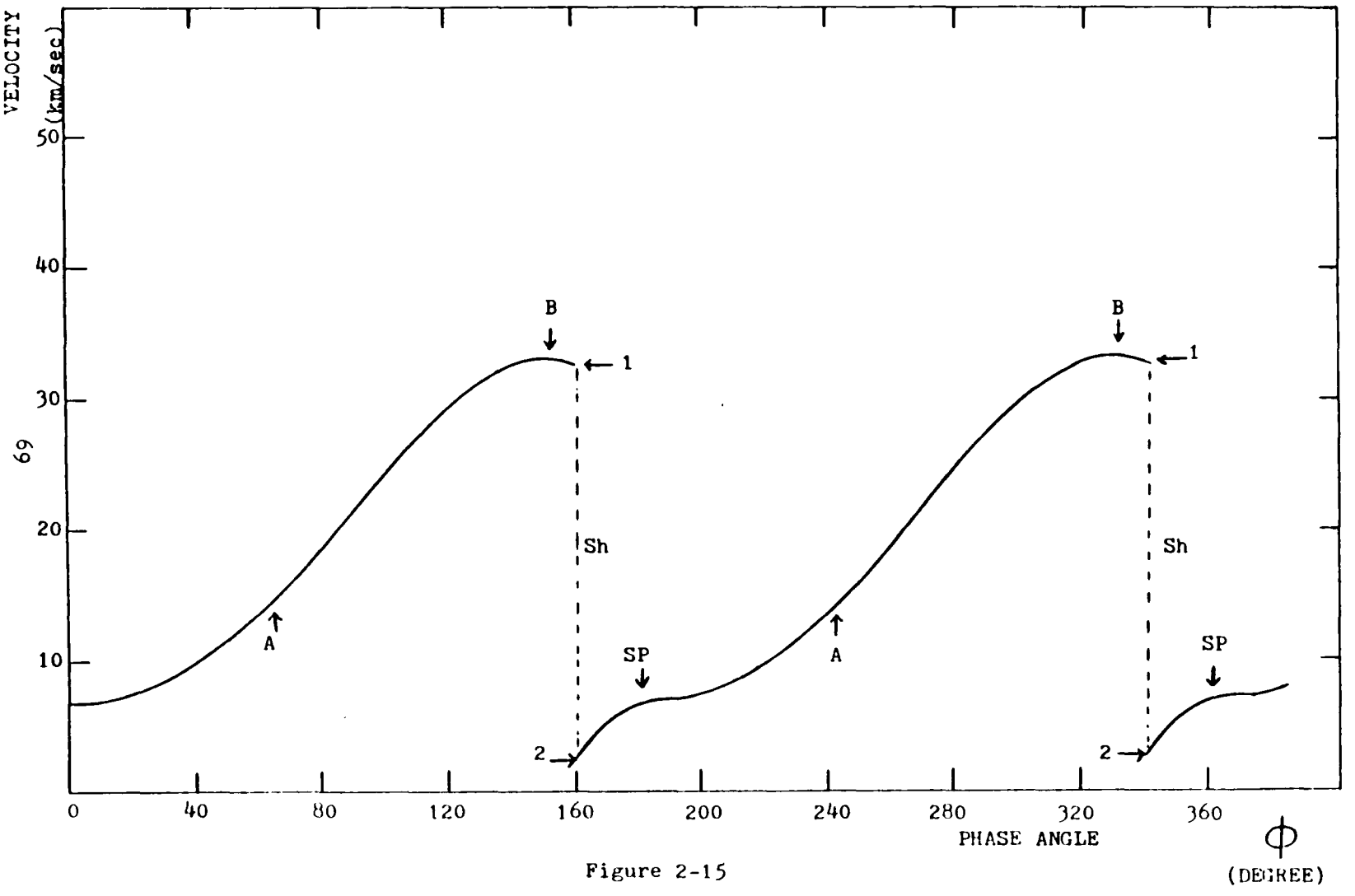
VELOCITY
(km/sec)
50
40
30
20
10
B
1
A
Sh
SP
2
B
1
A
Sh
SP
2
0
40
80
120
160
200
240
280
320
360
PHASE ANGLE
Φ
(DEGREE)

Figure 2-15

Figure 2-16: The variation of the pressure of the interstellar gas along the entire streamline which passes through the solar neighborhood.(De Jong's model)

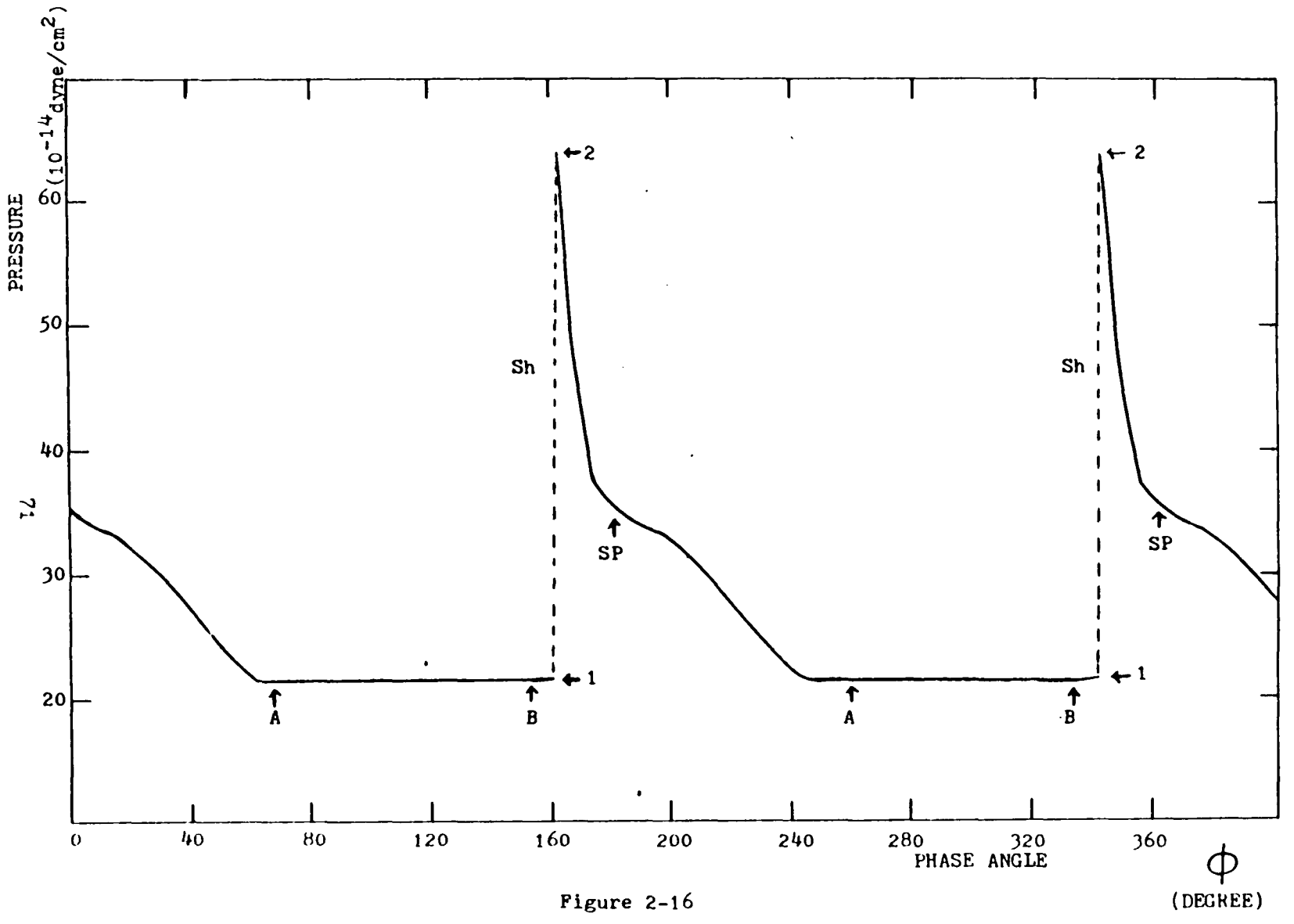
PRESSURE (10^-14 dyne/cm^2)
60
50
40
30
20
Sh
Sh
←2
←2
←1
←1
SP
SP
A
B
A
B
0
40
80
120
160
200
240
280
320
360
PHASE ANGLE
(DEGREE)

Figure 2-16

Figure 2-17: The variation of the number density of the intercloud medium along the entire streamline. (De Jong's model)

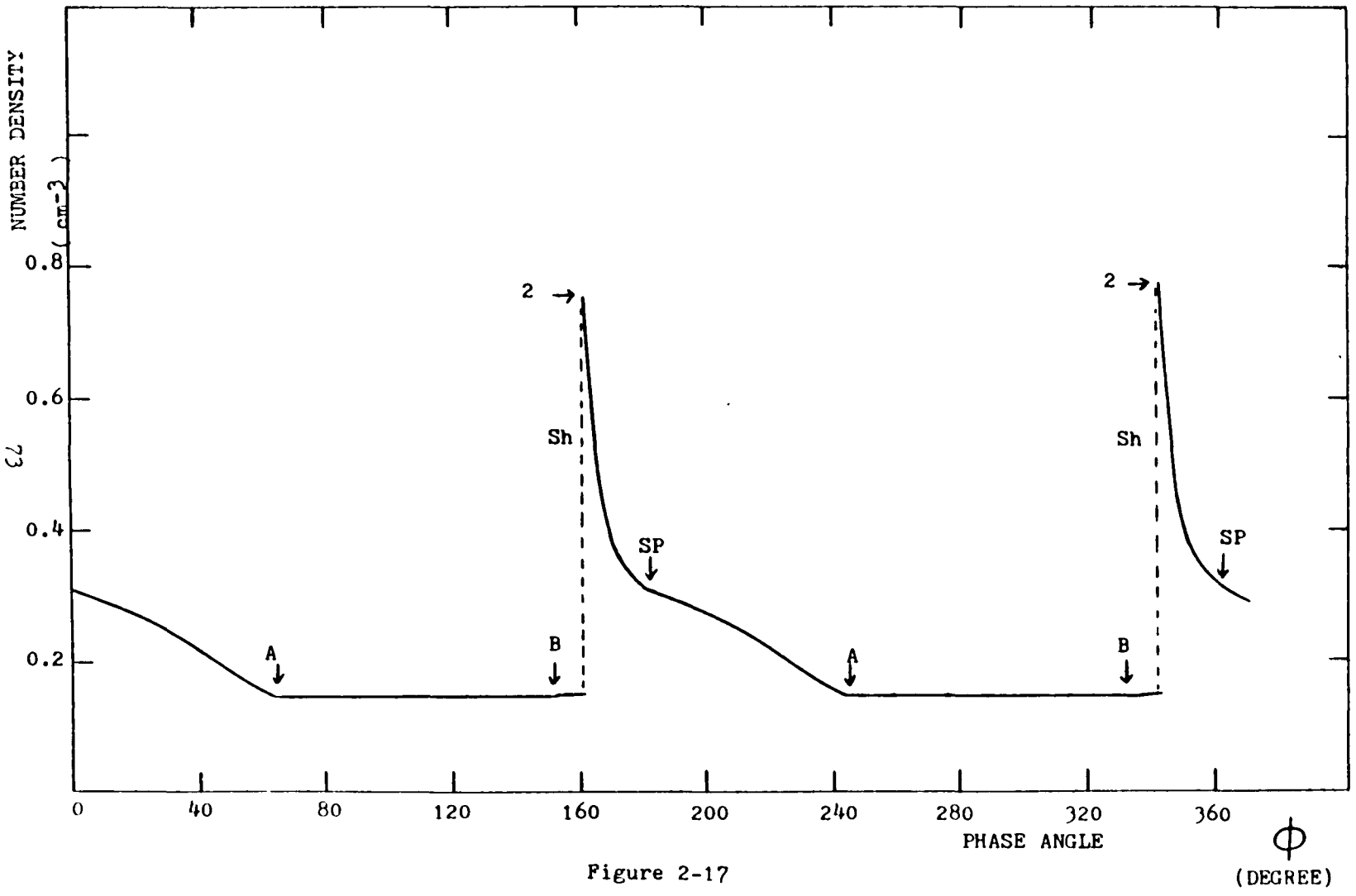
NUMBER DENSITY
(cm-3)
0.8
0.6
0.4
0.2
2
Sh
SP
A
B
2
Sh
SP
A
B
0
40
80
120
160
200
240
280
320
360
PHASE ANGLE
Φ
(DEGREE)

Figure 2-17

Figure 2-18: the variation of the local fraction of volume occupied by the cloud medium F_c along the entire streamline.(De Jong's model)

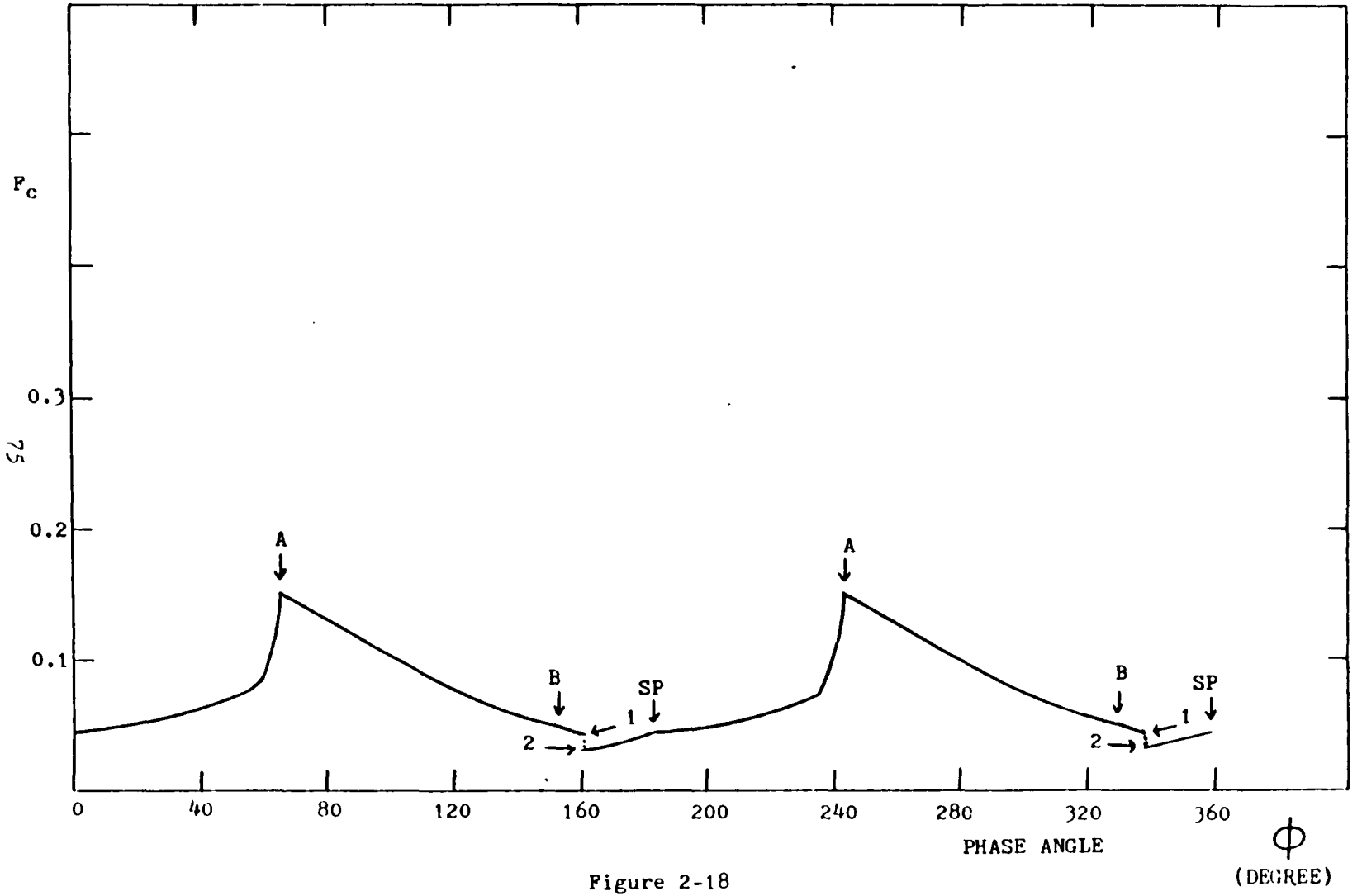
F_c
0.3
0.2
0.1
A
B
SP
1
2
A
B
SP
1
2
0
40
80
120
160
200
240
280
320
360
PHASE ANGLE
Φ
(DEGREE)

Figure 2-18

Figure 2-19: The variation of the radius of the entire streamline which passes through the solar neighborhood. (De Jong's model)

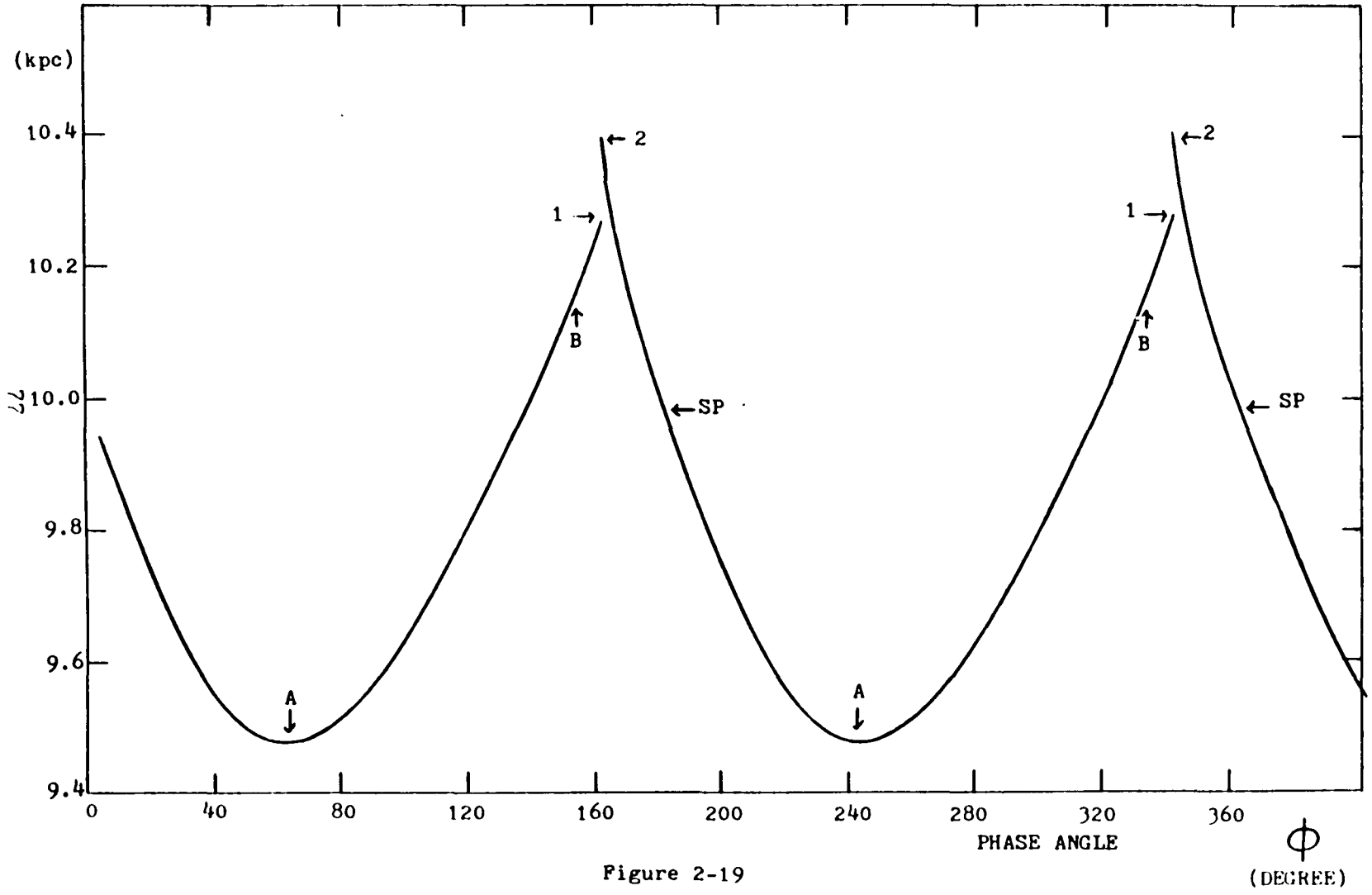
(kpc)
10.4
10.2
10.0
9.8
9.6
9.4
r
0
40
80
120
160
200
240
280
320
360
PHASE ANGLE
Φ
(DEGREE)
1
2
A
B
SP

Figure 2-19

CHAPTER III

THE INABILITY OF THE DRAG FORCE IN DECELERATING THE CLOUD MEDIUM

We demonstrate that the drag force between the cloud medium and the intercloud medium is not capable of slowing down the cloud medium so as to achieve the co-moving with the intercloud medium within a short distance behind the shock front. However, the existing observations strongly suggest that co-movement is achieved in a short distance behind the shock front. Therefore, we conclude that there must exist an effective mechanism which rapidly decelerates the cloud medium behind the shock front. We then suggest that the sudden deceleration of the cloud medium may be achieved through cloud-cloud collisions.

We follow the formulations of Shu et al.(1972) and Roberts(1969) closely and add the drag term to the governing equations. In addition to the study of the intercloud phase, our studies extend into the cloud phase for a further understanding of its dynamic behavior immediately behind the shock front. The governing asymptotic equations which include phase transition for the gas flow of cloud and intercloud phases in the postshock regions are the following four equations

$$\frac{dU_\eta'}{d\eta} = \frac{U_\eta \varpi \left\{ 2\Omega U_\xi + g_1 + \left(\frac{D}{\rho}\right)\left\{\frac{(U_{c\eta} - U_\eta)}{(1-F_c)}\right\}\right\}}{U_\eta^2 - a^2}, \tag{3-1}$$

$$\frac{dU_\xi'}{d\eta} = \frac{-\varpi \left\{ \left(\frac{K^2}{2\Omega}\right) U_\eta' + \left(\frac{D}{\rho}\right)\left[\frac{(U_{c\xi} - U_\xi)}{(1-F_c)}\right]\right\}}{U_\eta}, \tag{3-2}$$

$$\frac{dU_{c\eta}'}{d\eta} = \frac{\varpi U_{c\eta}\left[2\Omega U_{c\xi}' + g_1 - \left(\frac{D}{\rho_c}\right)\left(\frac{1}{F_c}\right)(U_{c\eta} - U_\eta)\right]}{U_{c\eta}^2 - C^2}, \tag{3-3}$$

$$\frac{dU_{c\xi}'}{d\eta} = \frac{-\varpi\left[\left(\frac{K^2}{2\Omega}\right) U_{c\eta}' + \left(\frac{D}{\rho_c}\right)\left(\frac{1}{F_c}\right)(U_{c\xi} - U_\xi)\right]}{U_{c\eta}}. \tag{3-4}$$

The last term in equations (3-1)—(3-4) is the drag term D which represents the drag force acting on the cloud medium per unit volume. The value of the drag term D strongly depends on the relative velocity of the cloud and its ambient intercloud medium. If the relative velocity is small, the drag force F_D can be approximated by the Stokes formula.

$$F_{DS} = 6\pi \langle R_c \rangle \mu (u - u_c), \qquad (3\text{-}5)$$

where $\mu = \rho\nu$ is the dynamic viscosity, and $\langle R_c \rangle$ is the average radius of the clouds. If the relative velocity increases, the Stokes formula is no longer valid. Instead the drag force is best described by an empirical equation.

$$F_{DE} = C_D \cdot \frac{1}{2} \rho \pi \langle R_c \rangle^2 |u - u_c|(u - u_c) \qquad (3\text{-}6)$$

The constant C_D depends on the shape of the object being tested and the Mach number of the relative velocity between the two media. For a rigid sphere, C_D increases linearly with the Mach number and becomes the constant 1 as the Mach number becomes greater than 1 (Hodges 1957; Chernyi 1961).

Despite the fact that a serious deformation of clouds may occur in the postshock regions, we should assume for simplicity that the clouds are spheres and that the volume of a cloud is $V_c = \frac{4\pi}{3} R_c^3$.

Therefore, the drag force per unit volume acting on the cloud medium is $D = F_D / V_c$.

$$D = \frac{3}{8} C_D \left(\frac{\rho}{\rho_c} \right) \frac{|u - u_c|(u - u_c)}{\langle R_c \rangle} \quad (3\text{-}7)$$

The motions of intercloud medium and the cloud medium after the shock front, are governed by equations (3 — 1)———(3 — 4), provided that the drag force is the only means of deceleration. In our calculations we integrate the above four equations equations(3 — 1)——— (3 — 4) numerically so as to understand the motions of the two media, such as the rate of deceleration and the location where both media reach comoving again. We use the postshock values of the intercloud medium and the preshock values of the cloud medium as the initial values of our numerical integrations. Our results(see Figure 3-1) show that the drag force is not capable of slowing down

the cloud medium so as to achieve the comoving with the intercloud medium within a short distance behind the shock front. Similar results also can be reacned by following simple numerical estimations and physical arguments.Thus,we use the values of table 1 and table 2 (chapter IV), with C_D=0.2 and C=8.54km S^{-1}. Introducing the independent variable S(section IV—e), such that $ds=\omega d\eta$, from equation(3—3) we find that

$$\frac{du'_\eta}{dS} = -22.1 \text{ km s}^{-1}\text{kpc}^{-1}.$$

This means that it would take 1.2kpc for the cloud medium to slow down to normal postshock velocity of the intercloud medium. Moreover the normal velocity of the intercloud medium also has a negative gradient,

$$\frac{du'_\eta}{dS} = -5.59 \text{ km s}^{-1}\text{kpc}^{-1},$$

which results in the negative denominator of equation (3 -1). This means the drag force does not speed up the intercloud medium, the intercloud medium slows down further.Therefore it would take more than 1.2kpc for the cloud medium to reach comoving with the intercloud me-

dium. This result is not compatible with the observations.

The situation becomes even worse when the tangential component are taken into consideration. We substitute numerical values into equations(3—2) and (3—4), we find that $\frac{du'_{\xi}}{ds} = 105\ Km\ s^{-1} kpc^{-1}$ and $\frac{du_{c\xi}}{ds} = -9.15\ Km\ s^{-1} kpc^{-1}$. Therefore the tangential components of the velocity of the cloud and the intercloud media are departing from each other rapidly at the begining. However this departing rate will eventually be offset by the drag force. The process again would take a distance of the order of kiloparsecs to complete. And this is no guarantee that the location where the tangential components converge will coincide with that of the normal components. Another difficulty in this approach is the existence of a singularity for equation(3—3) at $u_{c\eta} = c$. Physically, we would require the numerator to vanish at the same time. But the value of the numerator is essentially fixed by the initial conditions and the choice of C_D. Such a condition cannot be predetermined.

The following result is one of the samples of the integrations of equations (3 -1)——(3 -4) (see Figure 3 -1). The intergrations start at the initial postshock conditions, where $U_{c\eta}$ =28.766km/sec, U_{η}=2.286km/sec, and U_{ξ}=-11.83km/sec. The integrations are carried out forward from the immediate shock front to the 60° phase angle after shock at an increment of 1° phase angle. As shown in Figure(3-1), $U_{c\eta}$ is steadily slowed down by the drag force. U_{η} is accelerated slowly at the begining. Later the drag term overcomes the combination of the gravitational force and the coriolis force. The normal component of the intercloud medium is then further slowed down by the drag force. U_{η}' become very small and equal to 0.029km/sec at the 60° phase angle. In the tangential direction, due to the coriolis force, $U_{c\xi}$ and U_{ξ} diverge from the begining and maintain a velocity difference of about 8km/sec throughout the integrations.

The above discussions demonstrate that the integrations of four equations(equations 3-1 — 3-4) cannot converge. Co-movement for both phases cannot be reached by drag force alone. However, the existing observations strongly suggest that co-movement is achieved in a short distance behind the shock front. Therefore, we conclude that there must exist a more effective mechanism immediately behind the shock front which is responsible for the sudden deceleration of the cloud medium. The only alternative we know of is the cloud-cloud collisions.In chapter IV we shall carry out the detailed mechanism of cloud-cloud collisions and prove that they are the dominating mechanism that slows down the cloud medium immediately behind the shock front. Before our discussion of cloud-cloud collisions, we will discuss further the results of Sawa(1975) and Woodward(1976). By taking only equations(3-3) into account,Sawa(1975) successfully reached co-movement for the cloud and the intercloud phases. However, his results could only be achieved by neglecting the diversified tangential velocity (equa-

tions 3-2 and 3-4). Moreover, he took Stokes drag term into account, which is not valid for a supersonic flow in the immediate postshock regions. Besides all those shortcomings, he was not aware of the fact that in a composite fluid the intercloud medium cannot be accelerated by the drag force, on the contrary, the intercloud medium is further decelerated by the drag force.

Woodward(1976) calculated that the deceleration rate of a standard cloud is 0.25km/sec^2 per million years. Using the drag force of equation (3-7) and applying the one-dimensional Newton's equation, we have

$$dU_\eta/dt = -\frac{3}{8} C_D \rho/\rho_c \, U^2/\langle R_c \rangle$$

Adopting the results in chapter II where U = 26.48km/sec, ρ =0.17788, and ρ_c =1.3352, we assume $R_c \simeq$ 10pc, and find that $C_D \simeq 0.2$.

This value is remarkably close to the experimental result in laboratories which is C_D=1 for Mach number greater than 1. Since the intercloud medium is drastically different from the air in laboratories, the cloud medium is

also drastically different from the rigid spheres in laboratories. For a highly deformable and compressible cloud, there is no reliable value for C_D available at the present time. We will consider that $C_D=0.2$ in our later calculations throughout this thesis. If we use this deceleration of $0.25 km/sec^2$ per million years, it would take over 100 million years to slow down the cloud medium with initial speed $U_{cy}=28.766 km/sec$ to match the intercloud medium at the direction normal to the spiral arm. This distance is about halfway to the next spiral arm and contradicts existing observations. Moreover, in the tangential direction the drag forces acting on both media would generate a large velocity gap before the two phases could begin to move together.

Figure 3-1: The deceleration of the cloud medium by drag force alone, and the variations of the velocities of both the cloud and the intercloud media, immediately behind the galactic shock front.

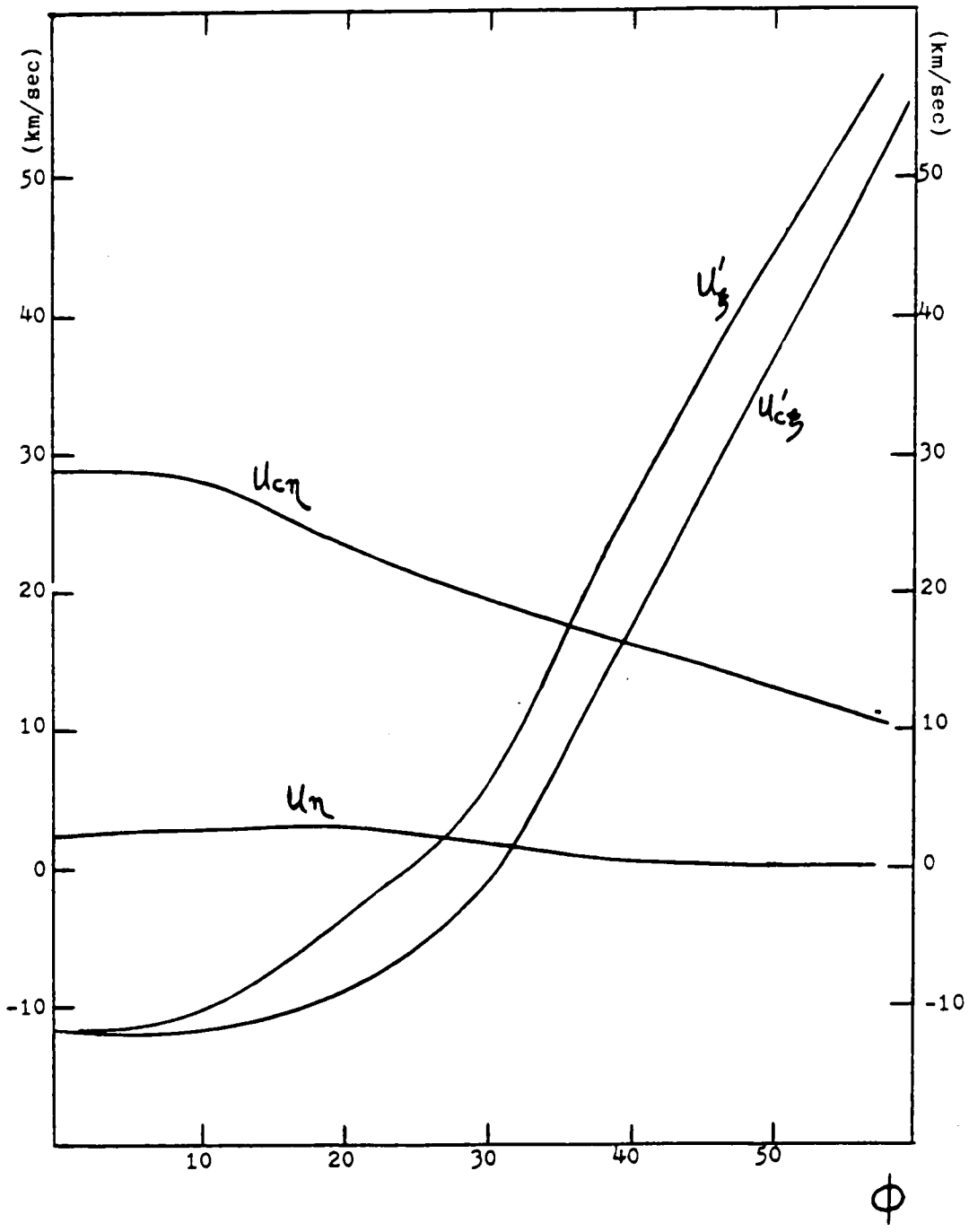
(km/sec)
50
40
30
20
10
0
-10
U'_ξ
$U'_{c\xi}$
$U_{c\eta}$
U_η
10
20
30
40
50
Φ
(DEGREE)

Figure 3-1

CHAPTER IV

THE SHOCK STRUCTURE OF THE CLOUD MEDUIM RESULTING FROM CLOUD-CLOUD COLLISIONS

In this chapter we demonstrate that the process of cloud-cloud collisions, which results in diffusive momentum transport and hence gives rise to the turbulent viscosity, is the main mechanism to decelerate the cloud medium behind the shock front. The governing equations with turbulent viscosity are derived. Then we analyze the internal structure of the galactic shock including the cloud medium. Our results show that the cloud medium also consists of its own viscous shock layer similar to that of the intercloud medium. The thickness of the shock of the cloud medium is determined to be of the order of 100pc. The shock layer of the cloud medium is formed immediately behind the shock of the intercloud medium which consists of a viscous layer of the order of 10^{-2}pc and is followed by a layer of phase transition and relaxation of the order of 20pc.

IV-a Structure of a Galactic Shock

The galactic shock can be divided into three layers as follows:

1. Viscous layer of the intercloud medium:

In this layer the atomic collisions redistribute the momentum and energy flux of the intercloud medium. For convenience, we assume the starting point of the viscous layer to be location 0 and the completion point of the viscous layer to be location 1. The thickness of this layer can be roughly estimated being of the order of the mean free path of atomic collisions.

2. Layer of thermodynamic relaxation and phase transition:

In this layer the intercloud medium undergoes the process of thermodynamic relaxation. Meanwhile the phase transition is taking place between the intercloud medium and cloud medium. We assume that this layer starts at location 1 and ends at location 2 which is the completion point of both thermodynamic relaxation and phase transition, although both processes may not be completed simultaneously. The

dimension of this layer can be roughly determined by the snowplowing process(see section IV-d). Since its thickness is of the same order of thermodynamic relaxation as estimated by Shu et al., we treat both processes in the same layer. At location 2 the galactic shock for the intercloud medium is completed.

3. The layer of cloud-cloud collisions:

In this layer the cloud medium plunges into the shock and suffers a serious deceleration via cloud-cloud collisions until the normal component of the velocity of the cloud medium matches that of the intercloud medium. There the galactic shocks are fully completed. We assume that the end of a galactic shock is location 3.

The thickness of this layer is of the same order of the mean free path of cloud-cloud collisions, which is estimated to be of the order of 100 pc.

The entire region from location 0 to location 3 is

defined here to be the complete galactic shock, which is the region where the "inner solution" is applied. This region was treated as an infinitesimally thin layer in the approach of Shu et al.(1972).

IV-b Final state of a galactic shock

The galactic shock is relatively thin compared to the entire field of the galactic flow. Therefore, the results of the final state of a galactic shock(at location 3) can be obtained by solving the following shock conditions——the conservation of mass and momentum. But energy is not conserved since heating and cooling takes place within this layer.

$$N_{c_3} U_{c\eta_3} = N_{c_0} U_{c\eta_0} + \Delta, \tag{4-1}$$

$$n_3 U_{\eta_3} = n_0 U_{\eta_0} - \Delta, \tag{4-2}$$

$$N_{c_3} U_{c\eta_3}^2 + n_3 U_{\eta_3}^2 + N_{c_3} C^2 + P_3/m_H = N_{c_0} U_{c\eta_0}^2 + n_0 U_{\eta_0}^2 + N_{c_0} C^2 + P_0/m_H, \tag{4-3}$$

where

$$N_{c3} = f_{c_3} n_{c_3} \quad , \quad \Delta = \frac{\delta_m}{m_H} . \tag{4-4}$$

In the above equations, δ_m is the mass flux involved in the phase transition, m_H is the mass of hydrogen atom; n_c is the number density of the cloud medium. f_c is the modified fractional volume of the cloud medium, which is defined in equation (2-18) as

$$f_c = \frac{F_c h_c}{(1-F_c)h} , \tag{4-5}$$

and h, h_c are the scale heights of the intercloud medium and the cloud medium. The numerical subscripts refer to the locations where the various quantities are taken. The equations of state of the intercloud medium can be represented by the following polytropic equation,

$$P = K \rho^{\gamma} \quad . \qquad (4-6)$$

In our calculation(chapter II), $K = 7500.$ and $\gamma = 0.675$. Using our results in chapter II for Shu's model, we can solve the algebraic equations(4-1)–(4-6). The upstream values at location 0 are listed in column 1 of Table 2. The downstream values at location 3 are listed in column 4 of Table 2. From our data in chapter II for De Jong's model, similar calculations are performed and the results are listed in Table 4. The graphical results are presented in Figure(4-1) for Shu's model and in Figure(4-2) for De-Jong's model.

IV-c The viscous layer

Like Shu et al., we treat this layer as a discontinuity. The exact thickness of this layer can not be determined unless we have better information concerning the viscosity, the thermal conductivity, and the p operties of atomic transport in the intercloud medium. Since it is the atomic collisions which are responsible for the energy and momentum redistribution in the intercloud medium, the thickness of the viscous layer must be of the order of the mean free path of the atomic collisions in the intercloud medium. Since the layer is so thin, the time scale is much shorter than the heating and cooling time. We will consider that the energy is approximately conserved in this layer. Therefore, the jump conditions for the discontinuity of the viscous layer must obey the following conditions (1) conservation of mass, (2) conservation of momentum, (3) conservation of energy, (4) conservation of electron mass, which corresponds to the following four algebraic equations:

$$n_1 u_{\eta_1} = n_0 u_{\eta_0} = j_0, \tag{4-7}$$

$$n_1 u_{\eta_1}^2 + \frac{P_1}{m_H} = n_0 u_{\eta_0}^2 + \frac{P_0}{m_H} = f_0, \tag{4-8}$$

$$\left(\frac{5}{2} f_0 - 2 j_0 u_{\eta_1}\right) u_{\eta_1} = \left(\frac{5}{2} f_0 - 2 j_0 u_{\eta_0}\right) u_{\eta_0}, \tag{4-9}$$

$$n_{e1} u_{\eta_1} = n_{e0} u_{\eta_0}. \tag{4-10}$$

We solve the algebraic equations (4-7)-(4-10), the results are presented in column 2 of Table 2. At location 1, the velocity of the intercloud medium slows down only halfway. Its velocity is still much higher than the postshock value u_η =2.483km/sec. Similarly, both the number density n_1=0.039cm^{-3} and the pressure of the intercloud medium have not yet reached their maximum values. The intercloud medium still must undergo the processes of thermodynamic relaxation and phase transition. As soon as both processes are completed, the intercloud medium will reach the final balanced state of a galactic shock.

IV-d The layer of thermodynamic relaxation and phase transition

Shu et al.(1972) studied in great detail the layer of thermodynamic relaxation for the case of F=0.033, which is a marginal case of a doubly-periodic shock solution without phase transition. The case of F=0.05 with phase transition, cannot yet be carried out in great detail due to insufficient information on the themodynamic functions required in the calculations such as heating, cooling, and ionization. Therefore, a precise thickness of the layer of relaxation with phase transition cannot be determined at the present time. However, its order of magnitude can be estimated through the study of the following process of phase transition called the "snowplowing" mechanism. Consider that a single cloud plunges into the shock of the intercloud medium at hypersonic speed. A bow shock will be formed in front of the cloud. Simultaneously, the sudden increase of its ambient pressure triggers an implosion wave which propa-

gates into the cloud. The pressure inside the bow shock is higher than its surrounding intercloud medium; if any phase transition is to take place, there must be a net condesation of mass from the intercloud medium onto the cloud within the bow shock. As the cloud plows through the intercloud medium, there is constantly a certain net amount of intercloud materials deposited onto the surface of the plowing cloud until phase transition ceases. By using the "snowplowing" mechanism, we can approximate the thickness of the layer of the phase transition, ℓ_{pt}, by using the following equation.

$$V_c = F_c(V_c+V_I) = n_s(4/3)\pi R_c^3 \ell_{pt} A . \qquad (4\text{-}11)$$

By taking $r = \Delta/(n_1 u_{\eta_1})$,

the amount of phase transition can be represented by

$$r V_I = r\frac{V_c(1-F_c)}{F_c} . \qquad (4\text{-}12)$$

In the above equation n_s is the number of clouds per unit volume, V_I is the volume of the intercloud medium, V_c is the volume of the cloud medium, and A is the cross section between the adjacent streamlines.

$$n_s(\ell_{pt} A).\pi(R_c')^2.\ \ell_{pt} = r V_c\frac{(1-F_c)}{F_c} , \qquad (4\text{-}13)$$

where the left-hand side of equation (4-13) represents the volume of the intercloud medium being snowplowed by the bow shock of the cloud, and R_c' is the effective radius of an average bow shock. Substituting equation (4-11) into equation (4-13) leads to the following result.

$$\ell_{pt} = 4/3 \frac{r(1-F_c)}{F_c} \left(\frac{R_c}{R_c'}\right)^2 R_c \qquad (4\text{-}14)$$

We arbitrarily assume that $R_c \simeq R_c'$ and R_c=8pc.

By using the result in Table 2,

where Δ=0.1258km S^{-1}, n_1=0.039cm^{-3}

U_{η_1} =13.5235km/sec, r=0.23597, and F_c=0.0856,

we can easily compute a crude estimate of the thickness of the phase transition layer ℓ_{pt}=26.89pc

However, if we assume that R_c'=1.5R_c, then ℓ_{pt}=12pc.

Thus the thickness of this layer depends heavily upon the strength and dimension of the bow shock in front of the cloud. We estimate that the actual value of the thickness of the layer of the phase transition may be somewhere be-

tween the above two values. It is probably in the neighborhood of 20pc.

Shu et al. (1972) determined the thickness of the layer of relaxation to be 50pc without phase transition. We do not know the detailed thermodynamic process within this layer; however, one effect we are sure about is that the phase transition provides an effective way of transporting the mass flux, momentum flux, and energy flux from the intercloud medium onto the cloud medium. The duration of the process of thermodynamic relaxation may be appreciably reduced in the presence of phase transition. Therefore, the thickness of the layer of relaxation will be considerably less than 50pc. In comparison with our result of the thickness of the layer of phase transition l_{pt}=20pc, we conclude that it is reasonable to state that the two processes actually overlap and enhance each other. Therefore, we treat those two processes together in our present calculations.

Although there is not enough information on this layer for us to acquire more accurate results, there is enough information for us to determine the final state of this layer(at location 2)using jump conditions.

$$n_2 u_{\eta 2} = n_1 u_{\eta 1} - \Delta \qquad (4\text{-}15)$$

$$N_2 u_{c\eta 2} = N_1 u_{c\eta 1} + \Delta \qquad (4\text{-}16)$$

$$n_2 u_{\eta 2}^2 + N_2 u_{c\eta 2}^2 + \frac{P_2}{m_H} + N_2 C^2 = n_1 u_{\eta 1}^2 + N_1 u_{c\eta 1}^2 + \frac{P_1}{m_H} + N_1 C^2 \qquad (4\text{-}17)$$

Again,this layer is very thin in comparison to the entire galactic flow field. It may be treated as a discontinuity. At location 2,the phase transition and thermodynamic relaxation ceases, and the thermodynamic equilibrium between heating and cooling processes is reached again in the intercloud medium. Therefore, in this case, the jump conditions conserve mass flux and momentum flux but not energy flux since the heating and cooling processes have already taken place before location 2.

Assuming that the cloud goes through the thin viscous layer without any change at all, we can say that $N_1=N_0$, $U_{c\eta_1} = U_{c\eta_0}$ while $P_2=K\rho_2^{\gamma}=K(n_2m_H)^{\gamma}$. The inter-cloud medium has already reached the balancing curve again at location 2 after relaxation and phase transition have been completed. There are four unknowns—N_2, n_2, U_{η_2}, and $U_{c\eta_2}$ in equations (4-15)——(4-17). We cannot solve those three equations unless we impose a condition to one of the four unknowns. Our results in the next section(IV—e) show that in order to solve equations(4-15)—(4-17), we must assume that $U_{\eta_2} = U_{\eta_3}$ =2.483km/sec. The numerical results are presented in column 3 of Table 2 for Shu's model and in column 3 of table 4 for De Jong's model.

IV-e The layer of cloud-cloud collisions

The last part of the galactic shock is composed of a thin layer of cloud medium embedded within a thermodynamically balanced intercloud medium. This layer is thin compared to the entire galactic flow field, but it is thicker than either the viscous layer or the layer of relaxation and phase transition. In this layer, the cloud medium loses most of its kinetic energy through its own internal friction, such as through the turbulent motion of clouds and cloud-cloud collisions. The magnitude of the effective kinematic viscosity in this process may be assumed to be the product of the mean free path of cloud-cloud collisions and the random turbulent speed of clouds C(ℓ =1xC). Spitzer (1968) estimated that the mean free path for standard clouds is about 100pc and the random velocity is about 8km S^{-1}. The kinematic viscosity therefore, is of the order of 1kpc-kmS^{-1}, which is much more effective than the drag force between the cloud medium and the intercloud medium. Thus in this section we

disregard the drag force and treat the cloud medium as a fluid which contains particles of individual clouds. As the cloud medium enters the high velocity gradient post-shock regions, particles of clouds pile up and slam into each other. Meanwhile, their kinetic energy is dissipated through cloud-cloud collisions and their own turbulent motions. Then the cloud medium slows down considerably and achieves co-movement with the intercloud medium within a reasonably short distance. We shall demonstrate in this section that the cloud medium will slow down and co-move with the intercloud medium within a short distance comparable to the mean free path of the cloud-cloud collisions. There the majority of the clouds will make one or more collisions with other clouds.

i) Governing equations

Using the same equations of Shu et al. (1972, p.566), we employ the Navier-Stokes equations for the intestellar medium in a rotating frame with the pattern speed Ω_p that may be expressed in the following forms:

$$\nabla\cdot(F_c\rho_c u_c) = \langle\dot{M}\rangle n_s \quad , \tag{4-18}$$

$$\nabla\cdot\left[(1-F_c)\rho u\right] = -\langle\dot{M}\rangle n_s \quad , \tag{4-19}$$

$$\nabla\cdot(F_c\langle\rho_c\rangle h_c u_c u_c) = F_c\rho_c\left[-\nabla(\mathcal{V}-1/2\Omega_p^2\varpi^2)-2\Omega_p x u_c+\tfrac{1}{3}\nu_c\nabla(\nabla\cdot u_c)+\nu_c\nabla^2 u_c\right]$$
$$-F_c\nabla(Ph)-Dh(u_c-u)+n_s h_c\langle\dot{M}v'\rangle \quad , \tag{4-20}$$

$$\nabla\cdot\left[(1-F_c)\,huu\right]=(1-F_c)\rho h\left[-\nabla(\mathcal{V}-1/2\Omega_p^2\varpi^2)-2\Omega_p x\, u\right]$$
$$-(1-F_c)\nabla(Ph)-Dh(u-u_c)-n_s h_c\langle\dot{M}v\rangle \quad , \tag{4-21}$$

where we assume that $h=h_c$ and that additional viscous terms $\frac{\nu_c\nabla(\nabla\cdot u_c)}{3}+\nu_c\nabla^2 u_c$ are included in equation (4-20) ν_c is the kinematic turbulent viscosity, where $\nu_c=\frac{\mu_c}{f_c\rho_c}$. μ_c is the effective viscosity in the postshock regions. The net momentum flux is only from the intercloud medium condensed onto the cloud medium. Therefore

$$n_s\langle\dot{M}v'\rangle = n_s\langle\dot{M}\rangle u \, .$$

Here we have to take few approximations similar to that of Shu et al.(1972) (1) $h=h_c$=constant (2) $(1-F_c)h$=constant (3) $F_c\nabla P$ is neglible compared to the other terms.

We then integrate equations (4-18)—(4-21) along the Z-direction adopting the logarithmic spiral coordinates (η , ξ) and applying the same asymptotic analysis of Roberts(1969). The results can be expressed as the following equations:

$$\frac{d}{d\eta}(\rho u_\eta) = -\epsilon\varpi \quad , \tag{4-22}$$

$$u_\eta \frac{du'_\xi}{d\eta} + \varpi\left(\frac{\kappa^2}{2\Omega}\right)u'_\eta = \frac{D\varpi}{(1-F_c)\rho}(u_{c\xi} - u_\xi), \tag{4-23}$$

$$u_\eta \frac{du'_\eta}{d\eta} - 2\varpi\Omega u'_\xi = -\frac{1}{\rho}\frac{dP}{d\eta} + g_1 + \frac{D\varpi(u_{c\eta} - u_\eta)}{(1-F_c)\rho}, \tag{4-24}$$

$$\frac{d}{d\eta}(\sigma_c u_{c\eta}) = \epsilon\varpi \quad , \qquad \sigma_c = f_c \rho_c , \tag{4-25}$$

$$u_{c\eta}\frac{du'_{c\xi}}{d\eta} + \varpi\left(\frac{\kappa^2}{2\Omega}\right)u'_{c\eta} = -\frac{D\varpi}{F_c\sigma_c}(u_{c\xi} - u_\xi) + \frac{\nu_c}{3\varpi}\frac{d^2u'_{c\xi}}{d\eta^2} + \frac{\epsilon\varpi}{\sigma_c}(u_\xi - u_{c\xi}), \tag{4-26}$$

$$u_{c\eta}\frac{du'_{c\eta}}{d\eta} - 2\varpi\Omega u'_{c\xi} = -\frac{c^2}{\sigma_c}\frac{d\sigma_c}{d\eta} + g_1 - \frac{D\varpi}{\sigma_c}(u_{c\eta} - u_\eta) + \frac{4}{3}\nu_c\frac{d^2u'_{c\eta}}{d\eta^2} + \frac{\epsilon\varpi}{\sigma_c}(u_\xi - u_{c\xi}), \tag{4-27}$$

where ϵ is the rate of the phase transition/unit length. If we assume ν_c is insignificant and negligible and that the clouds are co-moving with the intercloud medium, the above equations then reduce to the same equations as in Shu et al.(1972). The solution for those

equations is the solution for the "outer expansion". The "outer expansion" assumes that the cloud medium undergoes the same shock structure as the intercloud medium instead of going through its own shock layer via cloud-cloud collisions. However, at the present time, we will focus on the study of the behavior of the cloud medium within its own shock layer. These equations are usually referred to as "boundary-layer" type of equations or "inner expansion" in fluid mechanics. In this case, we have to treat the cloud medium as a flow containing many clouds. The drag force between the cloud and the intercloud media are negligible(D=0) inside the shock layer of the cloud medium. Therefore, the turbulent viscosity is the dominating force, while the gravitational force and the coriolis force are all negligible. The rate of phase transition in the layer is equal to zero. The above approximations can be reached through the following order of magnitude analysis.

ii) Order of magnitude analysis

In order to solve the "boundary-layer" type of equations, we must carry out an order of magnitude estimation of some important quantities in our calculations. First, we introduce an independent variable s, such that $ds = \omega_0 d\eta$, and a dimensionless quantity of small magnitude, δ, such that

$$(u'_\xi, u'_\eta, u'_{c\xi}, u'_{c\eta})/\omega_0(\Omega_0 - \Omega_p) = O(\delta) \quad , \tag{4-28}$$

$$\sin i = O(\delta) \quad , \tag{4-29}$$

$$s/\omega_0 = O(\delta^2) \quad , \tag{4-30}$$

$$\text{Reynolds number } R = O(\delta^{-2}) . \tag{4-31}$$

In order to demonstrate equation (4-30), we have to use the equation of continuity in full form for the cloud medium. (cf. equation, 4-25)

$$\frac{\partial}{\partial q}(\sigma_c u_{c\xi}) + \frac{\partial}{\partial s}(\sigma_c u_{c\eta}) - \sigma_c \frac{u_\xi \sin i}{\omega_0} + \sigma_c \frac{u_{c\eta} \cos i}{\omega_0} = 0 \tag{4-32}$$

where $dq = \omega_0 d\xi$ and the phase transition is equal to zero. We then divide equation (4-32) by $\sigma_{c2}(\Omega_0 - \Omega_p)$ and compare the order of magnitude of each of these terms. By arguing that the second term has to be one order of magnitude larger than the rest of the terms, we can easily reach the conclusion that s/ω_0 is at least $O(\delta^2)$.

Since $\varpi_0 \simeq$ 10kpc, s has to be of the order of 0.1kpc. This value is consistent with the thickness of the shock layer of the cloud medium estimated to be of the order of the mean free path of the cloud-cloud collisions. The Reynolds number R can be estimated by the following:

$$R = \varpi_0^2 (\Omega_0 - \Omega_p)/\nu_c$$
$$= \varpi_0^2 (\Omega_0 - \Omega_p)/C\times l \simeq 10^3$$

where l=0.1kpc , C=8.54kms^{-1} , ϖ_0=10.572kpc

and $(\Omega_c - \Omega_p)$=10.85km^{-1}s^{-1}kpc^{-1} (see table 1).

By comparing the orders of magnitude and neglecting smaller terms, equations (4-22)—(4-27) reduce to the following forms.

$$\frac{d(\rho u_\eta)}{ds} = 0 \qquad (4\text{-}32)$$

$$u_\eta \frac{d u'_\xi}{ds} = 0 \qquad (4\text{-}33)$$

$$u_\eta \frac{d u'_\eta}{ds} = 0 \qquad (4\text{-}34)$$

$$\frac{d}{ds}(\sigma_c u_{c\eta}) = 0 \qquad (4\text{-}35)$$

$$u_{c\eta} \frac{d u'_{c\xi}}{ds} = \frac{\nu_c}{3} \frac{d^2 u'_{c\xi}}{ds^2} \qquad (4\text{-}36)$$

$$u_{c\eta} \frac{d u'_{c\eta}}{ds} = -\frac{c^2}{\sigma_c} \frac{d\sigma_c}{ds} + \frac{4}{3}\nu_c \frac{d^2 u'_\eta}{ds^2} \qquad (4\text{-}37)$$

iii)Solutions to the "boundary-layer" equations

As a result of our approximations, the intercloud

medium is totally decoupled from the cloud medium and maintains a constant state throughout the shock layer of the cloud medium. $u'_\xi = u'_{\xi 2}$, $u_\eta = u_{\eta 2}$, $n = n_2$, $P = P_2$. (4-38)

Integrating equations(4-35)—(4-37)and assuming,

$$\frac{du'_{c\eta}}{ds} \approx \frac{d}{ds}(u^0_{c\eta} + u'_{c\eta}) = \frac{du_{c\eta}}{ds} .$$

we have the following results,

$$\sigma_c u_{c\eta} = \sigma_{c2} u_{c\eta 2} , \tag{4-39}$$

$$\frac{du'_{c\xi}}{ds} = \frac{3}{\mu_c}\sigma_c u_{c\eta}(u'_{c\xi} - u'_{c\xi 2}) + \left(\frac{du_{c\xi}}{ds}\right)_2 , \tag{4-40}$$

$$\frac{du_{c\eta}}{ds} = \frac{3}{4\mu_c}\left[\sigma_c u^2_{c\eta} - \sigma_{c2} u^2_{\eta 2} + (\sigma_c - \sigma_{c2})C^2\right] + \left(\frac{du_{c\eta}}{ds}\right)_2 \tag{4-41}$$

where the subscript 2 refers to location 2 at the end of the layer of the phase transition. Since $u_{c\eta}$ remains almost unchanged between location 0 and location 1, $u_{c\xi}$ is also unchanged between location 0 and location 1. Therefore $\left(\frac{du_{c\xi}}{ds}\right)_2$ and $\left(\frac{du_{c\eta}}{ds}\right)_2$ are both negligible in equations (4-40)and(4-41).By integrating equation(4-40),the following solution can be found,

$$u'_{c\xi} = u'_{c\xi_2} + C\, e^{\left(\frac{3u_{c\eta 2}}{4\nu_{c2}}\right)s} \tag{4-42}$$

The only physically possible solution for equation(4-42) is C=0. Equation(4-42)thus reduces to $u'_{c\xi} = u'_{c\xi_2}$.The tangential velocity for the cloud remains constant throughout this layer.We substitute equation(4-39)into equation(4-41), eliminate σ_c ,and recognize that $\nu_{c2} = \frac{\mu_{c2}}{\sigma_{c2}}$.

By introducing a new variable, $\zeta = \frac{3u_{c\eta 2}}{4\nu_{c2}} s$ (4-43)

equation (4-41) becomes

$$\frac{dU_{c\eta}}{d\zeta} = (U_{c\eta} - \frac{c^2}{U_{c\eta 2}})(1 - \frac{U_{c\eta 2}}{U_{c\eta}}). \qquad (4\text{-}44)$$

The solutions for equations (4-44) are such that upstream conditions should be $U_{c\eta} = U_{c\eta 2}$, while downstream conditions should be $U_{c\eta} = c^2/U_{c\eta 2}$.

Since $U_{c\eta 2}$=28.783km/sec(see table 1), we can easily find that $U_{c\eta 3}$=2.533kmS^{-1} although this value is slightly higher than the downstream value(at location 3) of the intercloud medium. However, this value is still within the limit of our approximation.

The solution of equation (4-44) can be written as

$$\zeta = \alpha_1 \ln(U_{c\eta} - U_{c\eta 2}) - \beta_1 \ln(U_{c\eta} - U_{c\eta 3}), \qquad (4\text{-}45)$$

$$\alpha_1 = \frac{U_{c\eta 2}}{U_{c\eta 2} - U_{c\eta 3}} = \frac{m^2}{m^2 - 1} \text{ and } \beta_1 = \frac{U_{c\eta 3}}{U_{c\eta 2} - U_{c\eta 3}} = \frac{1}{m^2 - 1},$$

where $m = U_{c\eta 2}/c$ is the ratio of the vertical velocity of the cloud medium and the random velocity of the cloud medium at location 2.

Assuming that $\mathcal{D}$ is the percentage drop of the velocity of the cloud medium within the layer of cloud-cloud collisions, we define $\mathcal{D}$ to be the following:

$$\mathcal{D} = \frac{u_{c\eta_2} - u_{c\eta}}{u_{c\eta_2} - u_{c\eta_3}} \times 100\% \qquad (4\text{-}46)$$

The thickness of the layer of cloud-cloud collisions, that is the "viscous" layer of cloud medium, depends heavily upon our chosen value of $\mathcal{D}$ as shown in Tables 5 and 6.

The results of our calculations are presented in the following section.

IV-f Results

Our calculations are based on two different models of two-phase interstellar gas as follows:

(1) The two-phase model of interstellar gas proposed by Shu et al.(1972), where the parameters are taken from our results in section II-a (shown in Table 1).

(2) The two-phase model of interstellar gas proposed by De Jong(1976), where the parameters are taken from our results in section II-c (shown in Table 3).

The results of ζ are determined from equation(4-45), and S is determined from the S, ζ relations of equation (4-43). The kinematic viscosity ν_{c_2} is equal to C x ℓ, and the mean free path of cloud-cloud collisions, ℓ is estimated by $(n_s \Sigma)^{-1}$. The number density of the clouds—— n_s is assumed to be $5 \times 10^{4} kpc^{-3}$(Spitzer 1968), and $\Sigma = \pi R_c^2$ is the average cross section of clouds. By taking R_c =10pc, ℓ is equal to 63pc in our calculations. The estimated thickness of viscous layer of cloud medium heavily depends upon the $\mathcal{D}$ value in equation(4-46). With the definition of $\mathcal{D}$ =99% the thickness of the viscous

layer for the cloud medium is equal to 152.566pc in Shu's model. By the same definition for De Jong's model the thickness of the viscous layer is equal to 213.514pc. If $\mathcal{D}$ is slightly reduced to 98%, the thickness of this layer decreases substantially to equal 132.478pc for Shu's model and 187.175pc for De Jong's model. If we use the definition of $\mathcal{D}$ =95% the thickness of the viscous layer for the cloud medium is further reduced to 100.6pc and 125.8368pc respectively. The detailed results are presented in table 5 for Shu's model and table 6 for De Jong's model. The value of N_c in table 5 and table 6 are determined by the equation(4-39). The overall changes of U_η, U_{c_η}, n, and N_c from the viscous layer to the layer of phase transition and relaxation and to the "viscous" cloud layer are presented in graphical form as shown in Fig. 1 for Shu's model with $\mathcal{D}$ =99% and in Fig.2 for De Jong's model with $\mathcal{D}$ =98%.

Figure(4-1) shows the overall distributions of the normal velocity and densities in galactic shock for Shu's

model. Between locations 0 and 1 is the viscous layer of the intercloud medium. Between locations 1 and 2 is the layer of relaxation and phase transition. While between locations 2 and 3 is the shock layer of cloud medium, with α =99%. The numerical results are based on Tables 1,2, and 5.

Figure (4-2) shows similar results to Figure (4-1) for De Jong's model, where α is equal to 98%. The numerical results are based on Tables 3, 4, and 5.

Figure 4-1: The variations of the normal velocities and densities in the galactic shock for Shu's model.

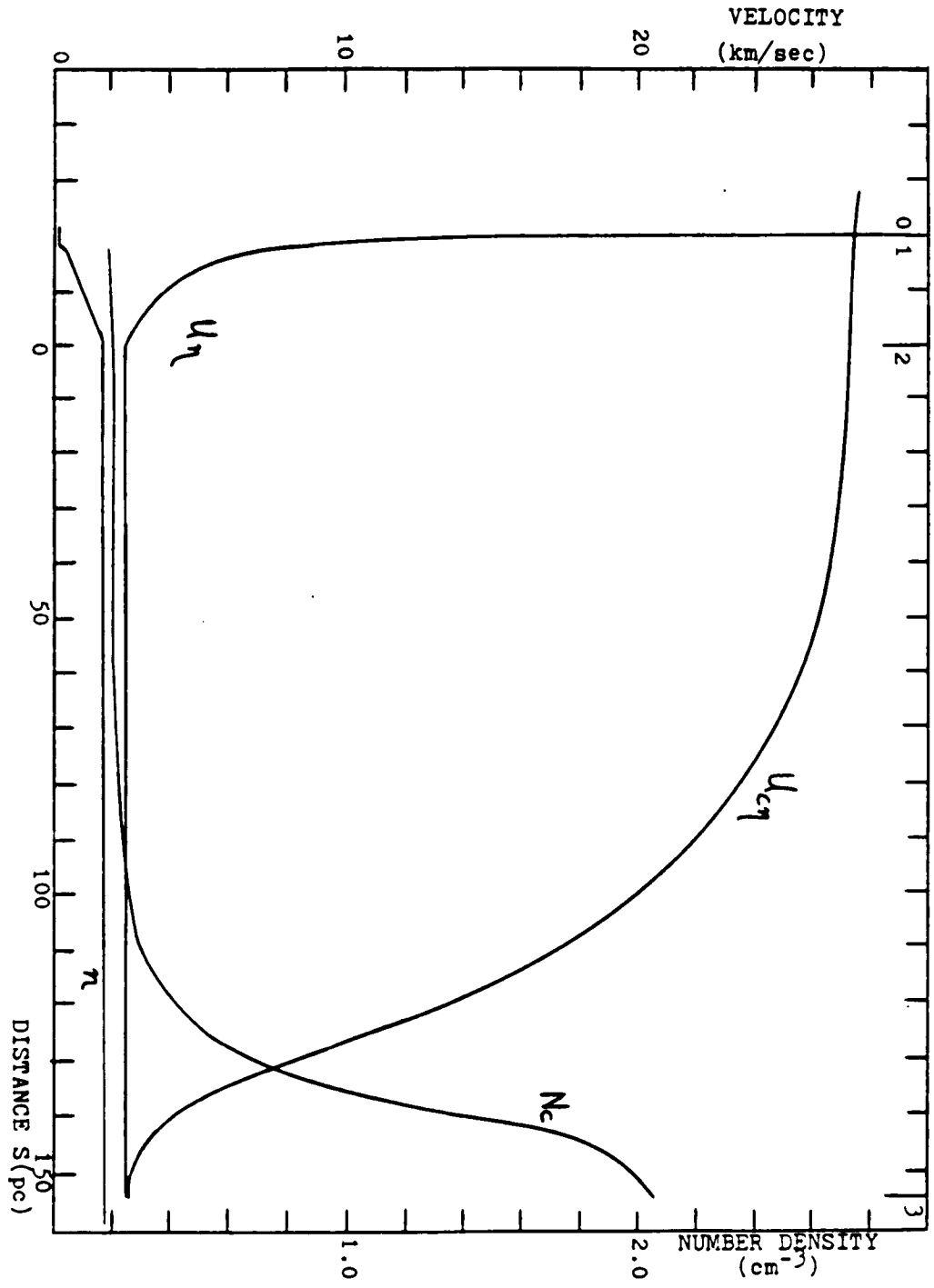
VELOCITY
(km/sec)
0
10
20
KEY LOCATIONS
0
1
2
3
u_η
$u_{c\eta}$
N_c
n
DISTANCE S(pc)
0
50
100
150
1.0
2.0
NUMBER DENSITY
(cm^{-3})

Figure 4-1

Figure 4-2: The variations of the normal velocities and densities in the galactic shock for De Jong's model.

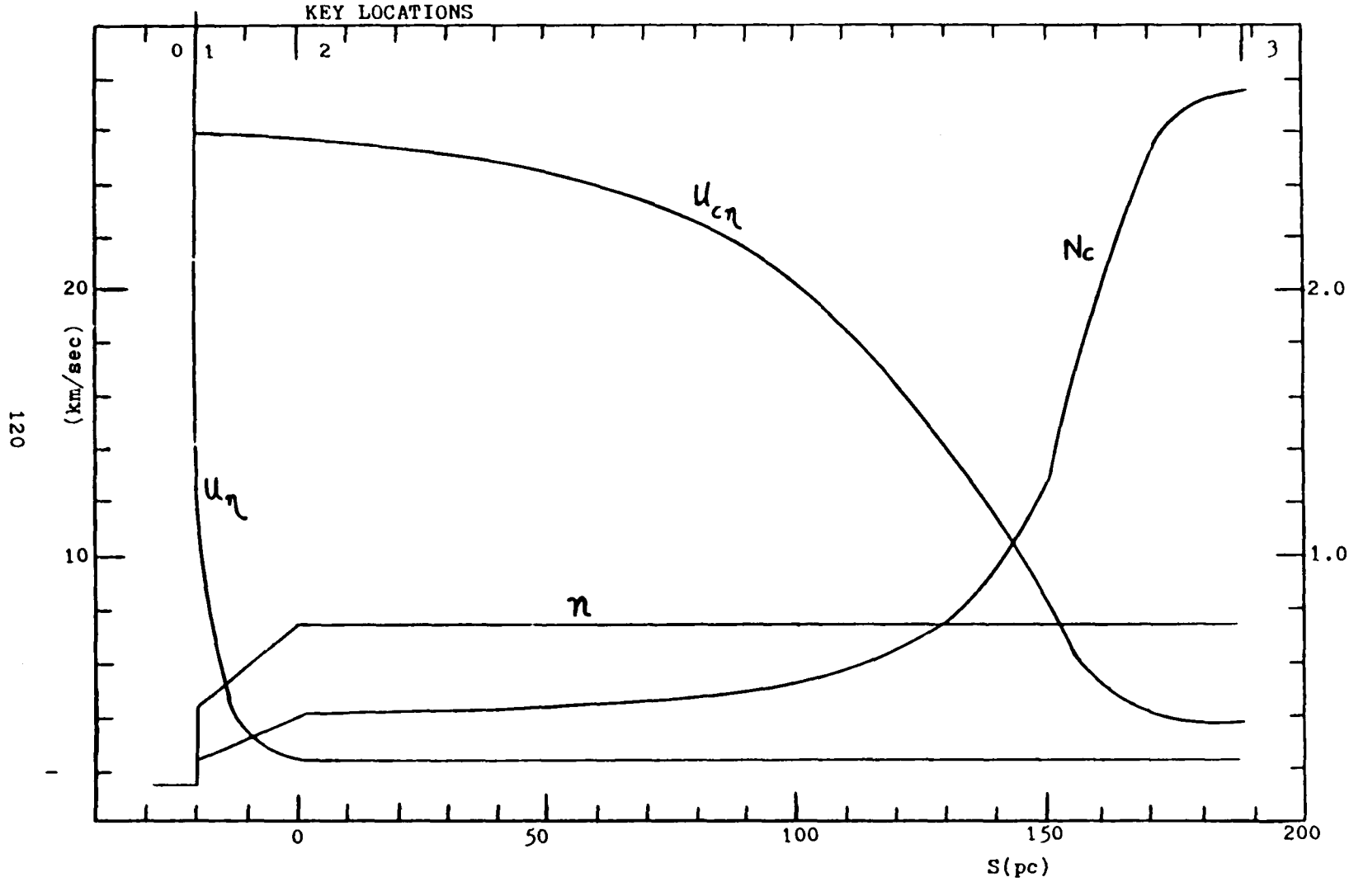
KEY LOCATIONS
0
1
2
3
$U_{c\eta}$
N_c
U_η
n
120
(km/sec)
20
10
2.0
1.0
0
50
100
150
200
S(pc)

Figure 4-2

TABLE 1

A GLOSSARY OF PARAMETERS USED IN THE COMPUTATION FOR SHU'S MODEL

ϖ_0 =10.57kpc	U_{ξ_0} = $U_{c\xi_0}$ =103.67km/sec
Ω_p =12.5km^{-1}s^{-1}kpc^{-1}	U_{η_0} = $U_{c\eta_0}$ =28.91km s^{-1}
Ω_0 =24.338km^{-1}s^{-1}kpc^{-1}	n_0 =0.018529
k =31.62km s^{-1}kpc^{-1}	n_{c_0} =1.3352
i =7	F_{c_0} =0.0856
U_ξ° = $U_{c\xi}^\circ$ =114.8km s^{-1}	log(p /k) =2.51684
U_η° = $U_{c\eta}^\circ$ =15.22km s^{-1}	Δ =0.0911km s^{-1}cm^{-3}
F =0.05	Φ =24

Note—The numerical values adopted in the present calculations are from chapter II. The subscript zero denotes the values taken just before the flow enters the shock.(U_ξ° , U_η°) are the velocity components of the basic galactic flow, which equals $\varpi_0(\Omega_0-\Omega_p)(\cos i, \sin i)$, and i is the pitch angle of the spiral arms. The quantity Δ is the amount of phase transition, and F is the ratio of the strength of the spiral gravitational field and the mean field. Φ is the phase angle of the shock location relative to the potential minimum, whereas the positive sign indicates lying on the inner side of the potential minimum and the total phase angle between two spiral arms is 360°.

TABLE 2

NUMERICAL VALUES OF THE PRINCIPAL VARIABLES AT THE FOUR KEY LOCATIONS FOR SHU'S MODEL

	LOCATION			
VARIABLE	0	1	2	3
u_n(km s^{-1})	28.91	13.5235	2.483	2.483
u_{cn}(km s^{-1})	28.91	28.91	27.446	2.653
u_s(km s^{-1})	103.67	103.67	103.67	103.67
u_{cs}(km s^{-1})	103.67	103.67	103.67	103.67
n(cm^{-3})	0.0185	0.0394	0.1746	0.1746
n_c(cm^{-3})	2	2		
F_c	0.0856	0.0856		0.055
N_c	0.1846	0.1846	0.2000	2.38
log(p/k)	2.5168	3.1192	3.1796	3.1796
a (km/sec)	10.2485	8.8	6.8	6.8
c=8.54km/sec				

NOTE— Location 0 is the shock front of the intercloud medium. Location 1 is the border line between the viscous shock layer and the layer of phase transition and relaxation. Location 2 divides the phase transition layer and shock layer for the cloud medium. Location 3 is the exit position of the shock layer of the cloud medium, where the velocity of the cloud medium matches that of the intercloud medium. a is the sonic speed.

TABLE 3

A GLOSSARY OF PARAMETERS USED IN THE COMPUTATION FOR De JONG'S MODEL

R_0 =10.237kpc	$U_{\xi_0} = U_{c\xi_0}$ =112.21km s^{-1}
Ω_p=12.5km $s^{-1}kpc^{-1}$	$U_{\eta_0} = U_{c\eta_0}$ =32.198km s^{-1}
Ω_0=24.3148km $s^{-1}kpc^{-1}$	n_0 =0.1489
k=33.5km $s^{-1}kpc^{-1}$	n_{c_0}=5.5
i=5.65	F_c=0.0382
$U^*_\xi = U^*_{c\xi}$ =120.36km s^{-1}	log(p /k)=3.1873
$U^*_\eta = U^*_{c\eta}$ =11.91km s^{-1}	Δ =2.9841km $s^{-1}cm^{-3}$
C =10.00km s^{-1}	=20
F =0.06	=7.14km s^{-1}

NOTE——The numerical values adopted in the present calculations are from chapter II.The subscript zero denotes the values taken just before the flow enters the shock.(U^*_ξ , U^*_η) are the velocity components of the basic galactic flow, which equals $R_0(\Omega_0 - \Omega_p)(\cos i, \sin i)$, and i is the pitch angle of the spiral arms. The quantity Δ is the amount of phase transition, and F is the ratio of the strength of the spiral gravitational field and the mean field. ϕ is the phase angle of the shock location relative to the potential minimum, whereas the positive sign indicates lying on the inner side of the potential minimum and the total phase angle between two spiral arms is 360°.

TABLE 4

NUMERICAL VALUES OF THE PRINCIPAL VARIABLES AT THE FOUR KEY LOCATIONS FOR De JONG'S MODEL

	LOCATION			
VARIABLE	0	1	2	3
U_η(km s^{-1})	32.198	10.954	2.4168	2.4168
$U_{c\eta}$(km s^{-1})	32.198	32.198	26	3.846
U_ξ(km s^{-1})	112.21	112.21	112.21	112.21
$U_{c\xi}$(km s^{-1})	112.21	112.21	112.21	112.21
n	0.1489	0.4376	0.749	0.749
n_e	2	2		-
F_c	0.0382	0.0382		0.0330
N_c	0.2367	0.2367	0.408	3.3036
log(p/k)	3.187	3.6527	3.6875	3.6875
a(km s^{-1})	7.14	6.4	4.5	4.5

NOTE—Location 0 is the shock front of the intercloud medium. Location 1 is the border line between the viscous shock layer and the layer of phase transition and relaxation. Location 2 divides the phase transition layer and shock layer for the cloud medium. Location 3 is the exit position of the shock layer of the cloud medium, where the velocity of the cloud medium matches that of the intercloud medium. a is the sonic speed.

TABLE 5

NUMERICAL VALUES OF THE PRINCIPAL VARIABLES BEHIND SHOCK FRONT FOR SHU'S MODEL

$\mathcal{D}$ %	$U_{c\eta}$(kms^{-1})	S (pc)	N_c (cm^{-3})
1	27.1981	-49.3258	0.2018
2	26.9501	-29.2384	0.2037
5	26.2064	2.6348	0.2094
10	24.9667	17.3351	0.2198
20	22.4874	37.9646	0.2440
30	20.0081	50.0072	0.2743
40	17.5288	58.8296	0.3131
50	15.0495	65.798	0.3647
60	12.5702	71.6994	0.4366
70	10.0909	76.9664	0.5439
80	7.6116	81.9667	0.7211
90	5.1323	87.3173	1.0695
95	3.8927	90.8240	1.4100
99	2.9009	96.5269	1.8921
99.9	2.6778	103.2402	2.0497

NOTE——The numerical values in the present calculations are taken from Tables 1 and 2. $\mathcal{D}$ represent the various percentage drop of the normal velocity of the cloud medium at different locations within the viscous layer of cloud medium. $U_{c\eta}$ is the normal velocity of the cloud medium. Various S values represent the locations of cloud medium which corresponds to various values. The S values are determined from equation(4-43). While N_c represent the densities of the cloud medium at corresponding locations within the shock layer of the cloud medium.

TABLE 6

NUMERICAL VALUES OF THE PRINCIPAL VARIABLES BEHIND SHOCK FRONT FOR De Jong's MODEL

$\mathcal{D}$ %	U_{cn} (kms^{-1})	S (pc)	N_c (cm^{-3})
1	25.7785	-74.4665	0.4115
2	25.5569	-48.1277	0.4151
5	24.8923	-13.2107	0.4262
10	23.7846	13.3744	0.446
20	21.5692	40.4371	0.4918
30	19.3538	56.5927	0.5481
40	17.1384	63.3886	0.6190
50	14.922	77.8940	0.7109
60	12.7076	86.0694	0.8348
70	10.4922	93.5404	1.0110
80	8.2768	100.8885	1.2817
90	6.0614	108.1838	1.7501
95	4.9537	115.194	2.1414
99	4.0675	125.7884	2.6080
99.9	3.8682	139.0474	2.7424

NOTE——The numerical values in the present calculations are taken from tables 1 and 2. $\mathcal{D}$ represent the various percentage drop of the normal velocity of the cloud medium at different locations within the viscous layer of cloud medium. U_{cn} is the normal velocity of the cloud medium. Various S values represent the locations of cloud medium which corresponds to various values. The S values are determined from equation(4-43). While N_c represent the densities of the cloud medium at corresponding locations within the shock layer of the cloud medium.

CHAPTER V:CONCLUSIONS

Our results in this thesis may be summarized as follows: we confirm the results of Shu et al., with a different numerical scheme. We also adopt De Jong's model for two-phase interstellar gas and carry out similar calculations. Our results are again qualitatively consistent with those of Shu et al(1972).

In shaping the overall galactic flow patterns, the cloud medium only plays a secondary role. However due to its greater optical depth, the cloud medium is more prominent in observations than that of the intercloud medium, especially immediately behind the galactic shocks. In order to compare the theory with the observations, a detailed study of the motion of the cloud medium behind the galactic shock is indispensable. Unfortunately there is no complete theoretical study for the cloud medium

available to us at the present time. In the previous theoretical work of Shu et al. (1972), the motion of the cloud medium was simply assumed to be identical to that of the intercloud medium even in the immediate postshock regions. In order to attain a more reliable theoretical result, a detailed study of the motion of the cloud medium behind the galactic shock front is carried out in this thesis to close the gap in the work of Shu et al.

We show that the drag force between the cloud and the intercloud media is not enough to slow down the cloud medium in a short distance behind the shock front. However the existing observations clearly show that the cloud medium does slow down in a short distance behind the shock front. An alternative mechanism of cloud-cloud collisions is studied and it is shown that the process of the cloud-cloud collisions is capable of decelerating the cloud medium immediately behind the galactic shock front of the intercloud medium.

Our results show that the process of the cloud-cloud collisions, which give rise to the diffusive momentum transport and hence the turbulent viscosity, is responsible for the rapid deceleration of the cloud medium behind the galactic shock front. Similar to the intercloud medium, the cloud medium also forms a shock. We show that the thickness of the shock layer of cloud medium is of the order of 100pc, provided that the kinematic turbulence viscosity is equal to the procuct of C——the mean turbulent speed of the clouds, and ℓ ——the mean free path of the cloud-cloud collisions.

The complete galactic shock for both the intercloud and the cloud media are therefore constructed by three layers (1) The viscous layer of the intercloud medium with a thickness of the order of 10^{-2}pc; (2) The layer of thermodynamic relaxation and phase transition, the thickness of this layer is of the order of 20pc, within which the normal velocity and the pressure of the intercloud medium reach their postshock value; (3) The shock layer of the

cloud medium, with a thickness of the order of 100pc. Since the thickness of the shock layer of the cloud medium is so small as compared with the normal distance between spiral arms, it justifies the approch of the "outer solution" of Shu et al.(1972). Furthermore, the cloud medium also consists of a shocklike solution similar to that of the intercloud medium with a thickness of the order of 100pc, which justifies the work of Roberts(1972) and Visser(1978) who constructed the theoretical 21cm line "observations" by simply using the velocity field of the intercloud medium.

REFERENCES

Black, J. H., and Dalgarno, A. 1973, AP. J.(Letters), 184, L101.

Chernyi, G. G. 1961, Introduction to Hypersonic Flow (New York: Academic Press).

De Jong, T. 1976, Astr. AP., 55, 137.

Delgarno, A., and McCray, R. A. 1972, Ann. Rev. Astr. AP., 10, 375.

Field, G. B., Goldsmith, D. W., and Habing, H. J. 1969, AP. J. (Letters), 155, L149.

Fujimoto, M. 1966, in IAU Symposium 29, Nonstable Phenomena in Galaxies, ed. M. Arkeljan (Yerevan: Armenian Acad. Sci.), P. 453.

Hodges, A. J. 1957, J. Aero. Sci., 24, 755.

Kulsrud, R. M., and Cesarsky, C. J. 1971, Astrophys. (Letters), 8, 189.

Lighthill, M. J. 1956, in Surveys in Mechanics, ed. G. K. Batchelor and R. M. Davies (Cambridge: Cambridge University Press).

Lin, C. C., Yuan, C., and Roberts, W. W. 1978, Astr. AP., 69, 181.

Mathewson, D. S., van der Kruit, P. C., and Brouw, W. N. 1972, Astr. AP., 17, 461.

O'Donnell, E. J., Watson, W. D. 1974, AP. J., 191, 89.

Roberts, W. W. 1969, AP. J., 158, 123.

Roberts, W. W. 1972, AP. J., 173, 259.

Roberts, W. W., and Yuan, C. 1970, AP. J., 161, 877.

Sawa, T. 1975, Sci. Reports Tohoku Univ., 58, 13.

Shu, F. H., Milione, V., Gebel, W., Yuan, C., Goldsmith, D. W., and Roberts, W. W. 1972, AP. J., 172, 557.

Spitzer, L. 1968, Diffuse Matter in Space (New York: Interscience).

Spitzer, L., and Scott, E. H. 1969, AP. J., 158, 161.

Watson, W. D. 1972, AP. J. 176, 103 and 271.

Woodward, P. R. 1976, AP. J., 207, 484.

Visser, H. 1978, dissertation. University of Groningen.

Yuan, C., and Wang, C. Y. 1982, AP. J., 252, 508.